A review of natural materials for solar evaporation

R. Fillet, V. Nicolas, Vanessa Fierro, A. Celzard

A review of natural materials for solar evaporation

R. Fillet, V. Nicolas*, V. Fierro, A. Celzard*

Université de Lorraine, CNRS, IJL, F-88000 Epinal, France

*Corresponding Author: vincent.nicolas@univ-lorraine.fr

*Corresponding Author: alain.celzard@univ-lorraine.fr

Abstract

One way to harvest solar energy is to produce steam from liquid water. Steam can be used to provide freshwater even in a harsh environment, with extreme temperature and low groundwater supplies. It can also be extracted from polluted soil or water, purifying the water in the process at the same time. Water evaporation systems are energy effective, with efficiencies ranging from 60% to over 90%. Furthermore, they can be cost-effective and have a low environmental impact, using the right materials. In this article, we will review natural materials, mainly of biological origin, proposed for solar evaporation, from wood and plants to algae and other atypical biomass such as fungi or wastes such as pomelo peels, through gels and foams, raw or charred. Their evaporation effectiveness will be presented and discussed, as well as their energy efficiency. This timely review suggests the suitability of natural materials for this application and reports on the progress that has already been achieved, as well as on the advances that remain to be made to improve the performance of these low cost, low environmental impact but high performance systems.

Keywords: Natural materials; Steam generation; Water treatment; Low-energy-consumption; Solar energy

1. Introduction

Energy is an essential part of human life and development, whether it is used for industrial purposes, transport or basic needs such as the provision of food and water. Among the many ways of harvesting energy, the use of renewable energy has been the subject of research and industrial efforts. Solar energy is a promising renewable energy because the amount that hits planet earth every hour is higher than what is consumed by human activities over an entire year [1]. Electricity can be generated using photovoltaic panels, but the efficiency of these systems is low and the cells are expensive. Hence, recent research has focused on the use of heat generated by solar flux [2,3]. It is mainly used to heat water that can be applied to heating systems or to generate clean water from seawater or polluted water. Besides, the water can also be used with heat engines to generate electricity [4].

In this paper, the process of water evaporation discussed here consists of exposing a certain amount of water to solar radiation. Unlike boiling at 100°C under normal pressure conditions, evaporation can occur at any temperature. Evaporation is a slow endothermic process that takes place at the surface of water, so several criteria can accentuate the phenomena: the radiative heat absorbed by the surface, the evaporation area of the water or a humid material, the ambient humidity and the amount of heat transferred by convection. An example of this process is the drying of laundry. To allow the laundry to dry quickly, it is essential to hang it stretched, in a room with low ambient humidity or outdoors, exposed to the sun. If the laundry is not stretched or is hung in a cellar, it will take much longer to dry.

Several types of systems exist and use a variety of materials. Some of these water evaporation systems (WESs) were first fixed under the surface of water (see Erreur ! Source du renvoi introuvable.(a)). In these conditions, sunlight passes through the water and is converted into heat at the surface of a solar thermal conversion material (STCM), which gradually increases the temperature of bulk water. The disadvantage of this method is that it

behaves poorly under real circumstances, losing heat in the bulk of water and reflecting the light back to the environment [2,3]. Another type of WES uses particles with high photothermal properties and dispersed in water to achieve the same goal as the former system (see Erreur ! Source du renvoi introuvable.(b)), but with the same disadvantages. Therefore, a third type of WES, in which the STCM is placed on the surface of the water, using foam or a porous structure to float (see Erreur ! Source du renvoi introuvable.(c)), is more suitable for solar evaporation. By using surface treatment processes, such as carbonisation or coatings to allow high radiation heat transfer, these systems can achieve high energy efficiency (over 90%) and high evaporation rates. It is interesting to note that, with this kind of WES, only a small area (typically less than one square meter) is normally enough to generate the amount of water necessary for the average human requirement, which is approximatively 2.5 L per day. In the following, all the examples of WESs and STCMs that will be discussed will refer to the case (c) shown in **Fig. 1**.

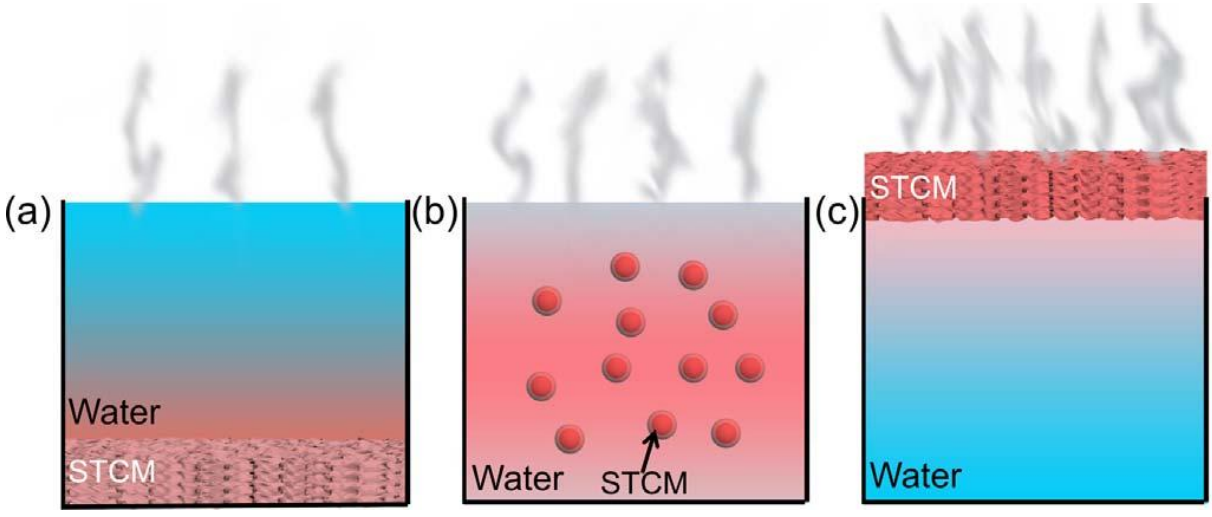

Fig. 1. (a) Different configurations of WESs, based on a solar thermal conversion material (STCM) either: (a) attached to the bottom; (b) dispersed in water; or (c) floating above the water. Reproduced from [2]. Copyright (2019), with permission from Elsevier.

To optimise the performance of STCMs, three main factors must be taken into account [2]: having a high solar absorbance, optimising the transport of water to the surface, and limiting thermal losses. To achieve high absorbance, treatment at the interface between the material

and the air is often performed. It is possible to use metallic nanoparticles [5,6], nanostructured semiconductors [7,8], or dark materials based on carbon [9,10] or on polymers [11,12].

Once the absorbance at the material surface is optimised, it is necessary to provide a constant flow of liquid water while retaining heat at the surface. The method used to improve the transport of liquid water to the surface is to use the capillary phenomenon of porous materials [13–15] and/or to use hydrophilic materials [16,17].

Finally, in order to design an efficient STCM, it is necessary to limit thermal losses. At the interface between the STCM and the air, the heat flux received by the absorber material consists of a thermal equilibrium depending on the solar flux received, the losses by convection and radiation, and the energy lost by the phase change of water (from liquid to vapour). Thus, this heat transfer can be written as follows:

$$\phi_t = \phi_{sun} + \phi_{conv;t} + \phi_{rad;t} + \phi_{l\to v} \quad (1)$$

$$\phi_t = \phi_{sun} + \underbrace{h_{c;t}\left(T_{\mathrm{inf};t} - T\right)}_{\phi_{conv;t}} + \underbrace{\varepsilon\sigma\left(T_{\mathrm{inf};t}^{\,4} - T^4\right)}_{\phi_{rad;t}} + \underbrace{\dot{m}_{tot} h_v}_{\phi_{l\to v}} \quad (2)$$

where ϕ_t is the total heat flux (W m^{-2}), ϕ_{sun} is the heat flux received from the sun (W m^{-2}), $\phi_{conv;t}$ is the convective heat flux (W m^{-2}) exchanged with the ambient temperature ($T_{\mathrm{inf};t}$ in °C), $h_{c;t}$ is the convective heat transfer coefficient (W m^{-2} K^{-1}), $\phi_{rad;t}$ is the radiative heat flux (W m^{-2}) exchanged with the ambient temperature ($T_{\mathrm{inf};t}$ in °C), ε is the emissivity of the material, σ is the Stefan-Boltzmann constant (kg s^{-3} K^{-4}), $\phi_{l\to v}$ is the heat flux due to the phase change of liquid water to vapour depending on the total vapour flux $\dot{m}_{tot}$ (kg m^{-2} s^{-1}), h_v is the sum of the enthalpy of vaporisation and the sensible heat (J kg^{-1}), and t is an index referring to the top of the absorber material.

At the bottom, there is heat transfer at the interface between the material and water. There are three main transfers: conduction, radiation and convection. The general heat transfer to the bottom of the water tank can then be written as follows:

$$\phi_b = \phi_{conv;b} + \phi_{rad;b} \quad (3)$$

$$\phi_b = \underbrace{h_{c;b}\left(T_{\text{inf};b} - T\right)}_{\phi_{conv;b}} + \underbrace{\varepsilon\sigma\left(T_{\text{inf};b}^{\,4} - T^4\right)}_{\phi_{rad;b}} \quad (4)$$

where ϕ_b is the total heat flux (W m^{-2}), $\phi_{conv;b}$ is the convective heat flux (W m^{-2}) exchanged with the bulk water ($T_{\text{inf};t}$ in °C), $h_{c;b}$ is the convective heat transfer coefficient (W m^{-2} K^{-1}), $\phi_{rad;b}$ is the radiative heat flux (W m^{-2}) exchanged with the bulk water ($T_{\text{inf};t}$ in °C), and *b* is an index referring to the bulk water.

At the top of the STCM, it is quite difficult to imagine a reduction in convection losses because they are directly related to vapour transfer. Indeed, the vapour is mainly transported by convection outwards. On the contrary, it is possible to limit radiation losses by applying a 3D radiation shield in the form of a cylinder at the top of the STCM [18]. Heat losses at the bottom are reduced by the use of thermal insulation (carbon foam or low-density wood, for instance) [19] or by designing an air volume inside the system [20].

There are already several review articles concerning this type of systems [2,3,5,21,22], but these former reviews mainly report on the strategies used to improve WESs in a very general way, in particular through the design of steam-to-liquid water conversion systems based on all types of materials without restriction, and discuss their potential applications. In this very general case, the materials used can be synthetic or natural (biological or mineral). Thus, as explained above, absorbers can be composed of metallic nanoparticles, nanostructured semiconductors or dark materials based on carbon or polymers, the latter two leaving many possibilities for the use of biological materials.

Insulating materials to limit heat transfer to water can be made from polyurethane foam [23], porous carbon [10], expanded polystyrene [9,14,18,24–28] or natural materials such as wood [19,29,30] and its derivatives [31], or even simply air [20]. Concerning the transport of liquid water, bio-based materials are often suggested. In general, WESs are made of several materials, whether bio-based or not, and bio-based materials do not necessarily result in lower performance compared to their synthetic counterparts.

This paper will cover the variety of WESs that use natural materials, the vast majority of them bio-based, and explain how their particular characteristics can benefit solar evaporation. Many natural structures found in nature, especially biologic species, can indeed be a source of inspiration and studies have already been inspired by features present in nature. First, it will be explained how the performance of a given WES can be measured, and the different quantities and notations required will be defined. These will be referred to throughout the following when comparing the efficiency of the systems with each other. Then, the main strategies to improve the evaporation rate will be explained and linked to the specific characteristics of different materials. Finally, evaporation rates and other results obtained using bio-based and other natural materials will be presented, as well as prototypes existing to date.

2. General information on solar water evaporation

2.1. Measurement process and definitions

Solar water evaporation measurements are usually conducted using a solar light simulator, most often with a xenon lamp that simulates the sunlight spectrum very well. In a typical experiment, a container filled with water and including the evaporation device according to its design, is then placed under the lamp and on an electronic balance. The illumination is set to a chosen value, which is usually a multiple of 1 sun (e.g. 1, 3 or 10 suns). 1 sun represents an

irradiation with a power density of 1 kW m^{-2}, i.e., the average photonic energy flux through the atmosphere at an altitude close to sea level. Although the simulator can be set to several output powers, in real conditions, optical devices or lenses can be used to achieve a power density higher than 1 kW m^{-2}. The balance, ideally coupled to a continuous data logging system, then measures any water loss over the period under consideration. From this loss, the evaporation rate (ER) can be calculated with the common unit found in the literature: kg m^{-2} h^{-1}.

In order to quantify the performance of WESs, almost all of the work reviewed on this topic reports efficiency values, most often calculated using the following equation:

$$\eta = \frac{\dot{m} h_v}{C_{opt} P_0} \quad (5)$$

where η if the efficiency (dimensionless, but more often expressed in %), $\dot{m}$ is the net evaporation rate (i.e., the evaporation rate only due to light) in kg m^{-2} h^{-1}, h_v is the sum of the enthalpy of vaporisation and sensible heat (J kg^{-1}), C_{opt} is the optical concentration of the solar flux, and P_0 is the power density of the solar flux, usually reported in sun number (equivalent to 1 kW m^{-2}). To compare the capacity of water evaporation systems, it is preferable to use the evaporation rate rather than the efficiency, as the latter can be calculated in different ways so that, in some cases, systems with comparable efficiencies may have significantly different ERs from each other [32,33].

Indeed, depending on the system used to test the material and on the experimental conditions, the energy balance is likely to change from one test to another [34]. As one study [35] pointed out, if the temperature of the system is lower than the temperature of the environment, heat transfer occurs from the environment to the system, adding energy to it. This energy is not taken into account when using Equation (5), and most publications do not mention it. Moreover, if the vessel containing the water to be evaporated is not insulated, the

diffuse radiation increases the evaporation rate without being taken into account in the efficiency calculation, resulting in a higher efficiency value. For instance, it has been reported that the efficiency of a wood-polydopamine system increased from 87% when exposed to 1 sun to 135% when exposed to 3.5 sun [36]. In general, Equation (5) is used in many reviews but has limitations, as the efficiency can never be greater than 100%.

2.2. Main characteristics of water evaporation systems

Exposing bulk water to solar radiation allows the water to extract energy from sunlight, even if part of this energy is lost in the process. Part of the light is indeed reflected back to the environment, resulting in less energy being gained by the system. Moreover, the system will have a different temperature than the environment, which will allow heat transfer from one to the other, usually from the WES, resulting in energy losses.

The first way by which studies have tried to remedy these losses has been to adjust the amount of solar energy absorbed and transferred to the water. The ideal situation is therefore when most of the energy is absorbed and nothing is returned to the environment. This can be achieved by using a surface with a high absorbance over the entire solar spectrum, either by being dark (such as carbon) or by having special semiconducting or plasmonic properties (such as titanium-based compounds and metallic nanoparticles, respectively), which results in high photothermal properties. Another source of losses in WESs is the heat that is given to bulk water (i.e., not retained on the surface) and then returned to the environment by thermal conduction. To minimise this, most devices use materials with low thermal conductivity. A material with low thermal conductivity means that less energy will be lost in contact with bulk water and, since evaporation is a superficial phenomenon, the WES has the advantage of retaining as much heat as possible at the surface. However, this is only possible if the water

has actually reached the surface where evaporation takes place. Therefore, water transport is another characteristic to be taken into account when designing evaporation systems.

Bio-based materials are especially well suited for water transport because this is precisely the function of most of them in nature. The sapwood for example, through its vessels or tracheids, is used to supply sap from the bottom of the tree to the top. Similarly, rice straws have a spiral geometry that allows an upward capillarity effect [37]. In general, many natural materials are both porous and hydrophilic. These characteristics allow them to combine a character of thermal insulation (given the very low thermal conductivity of air, 0.026 W m^{-1} K^{-1} at room temperature) with a capacity to transport water within them. It is therefore not surprising that this type of material has been suggested as the core of devices for solar WESs, and the following section reports many examples of this type of materials, which are now detailed and discussed. Unless otherwise stated, the data reported below in terms of evaporation rate and efficiency were obtained under a solar irradiation equivalent to 1 sun. When the photonic energy was higher, the evaporation rate corresponding to 1 sun was calculated assuming proportionality. More details are given below.

3. Review of natural materials for solar evaporation

In the following, materials reported as efficient cores for solar water evaporation systems have been classified according to their origin and, to some extent but not completely, according to their structure. As with any classification, it is not completely satisfactory, as there are always materials that do not fall into any category, and which should be listed in an "other natural materials" subsection. But any other classification of materials, whether based on their structure, nature or function, always leads to the same imperfections. We have therefore chosen to present them by major types of natural resources, mainly plant resources, with special emphasis on the treatments carried out. Indeed, depending on whether the

biomass is used in its raw state or after carbonisation, giving what is called a biochar, the resulting materials are very different. They will nevertheless appear in the same sections, as they come from the same raw material.

3.1. Wood-based materials

Wood is the structural material of trees, which also provide them with capillary capacity to feed sap to the leaves. While there are more than twenty thousand species, only a handful of them are actually used regularly for their mechanical properties for structural purposes or for making furniture. Its solar evaporation capacities have been explored by numerous studies to date.

3.1.1. Main characteristics of wood

Wood consists of approximately 45% cellulose, 30% hemicellulose and 25% lignin. These numbers may vary whether it is hardwood or softwood, and depending on the species. Cellulose is a homopolymer of glucose while hemicellulose is an amorphous heteropolymer of polysaccharides. This means that wood has many hydroxyl groups, which are very hydrophilic. Softwood has two main types of cells, parenchyma cells and tracheids. The latter are used as mechanical support and for sap transport. Hardwood, on the other hand, has an additional type of cells specially designed for this task, the vessels. Both softwood and hardwood have ligneous rays that provide additional porosity from the centre of the trunk to the outside.

Most woods have a lower density than water, which allows them to float on it. Some are atypical, for instance balsa has a remarkably low density of 200 kg m^{-3}. Softwoods have an average density of 400 to 500 kg m^{-3} while hardwoods have a density ranging from 600 to 800 kg m^{-3} (**Fig. 2**). As mentioned above, thermal insulation plays a major role in WESs. Wood

meets this criterion by having a thermal conductivity ranging from 0.1 to 0.5 W m^{-1} K^{-1} depending on the species [38,39] and the direction of the fibres [40].

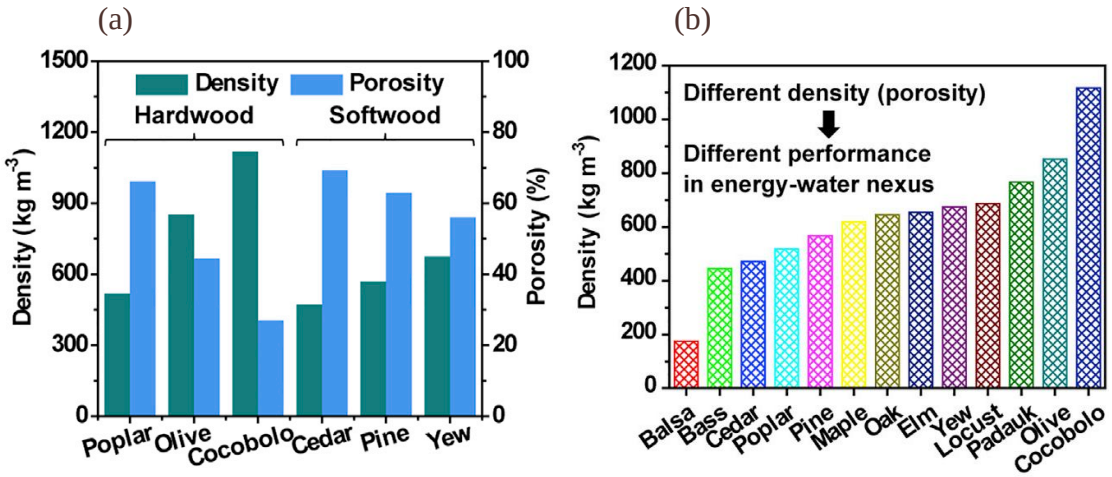

Fig. 2. (a) Density and porosity of different types of woods; (b) Density of several wood species. Reproduced from [41]. Copyright (2017), with permission from Elsevier.

3.1.2. Wood with coatings

Naturally, wood is not a very light-absorbing material [42]. Therefore, a surface coating or process is required to achieve higher evaporation rates. Carbon-based materials such as carbon nanotubes (CNTs) [43], graphite [40] or graphene [44] have proven to be excellent light absorbers and are indeed present in many WESs, including those based on biomass. Chen's team obtained an evaporation rate as high as 11.22 kg m^{-2} h^{-1} under an irradiation equivalent to 10 suns for an efficiency of 81%, using balsa coated with CNTs [19]. Although the proportionality may not apply strictly because systems become more efficient as light intensity increases, this result suggests that the maximum ER calculated proportionally for 1 sun (MERCP1) would be 1.12 kg m^{-2} h^{-1}. In the following, for system-to-system comparison purposes, the notation "MERCP1" will be used to give a maximum ER value under 1 sun, calculated from measurements under more than 1 sun.

In addition to carbon, metals are also found as coatings on the surface of wood products [29,45,46]. These metals are sprayed as particles in a thin, controlled layer on the surface of wood. Tannic acid – Fe^{3+} complexes were also found to present good photothermal properties,

without the need for high temperatures in their preparation [38]. In fact, based on the results of evaporation rates, this type of coating performed better than others did, with an ER of 1.85 kg m^{-2} h^{-1} at 90% efficiency. Another coating that has been found to perform well when applied to wood is polydopamine (PDA), a polymer used by mussels to attach securely underwater. It should be noted that with a solar light intensity higher than 1 sun, wood products treated with PDA (**Fig. 3**) achieved an efficiency higher than 100% when calculated with Equation (5). The authors suggested that enthalpy is reduced in these systems, and that water evaporation is boosted by the formation of bubbles near the surface where boiling takes place, and therefore does not require so much energy input [36].

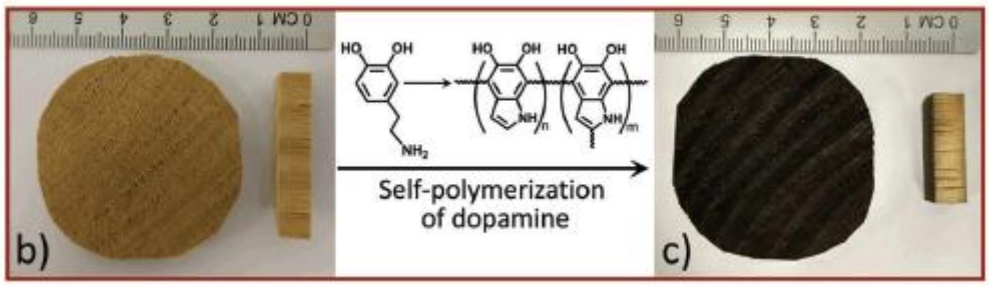

Fig. 3. Wood before (left) and after (right) applying a PDA coating .Reproduced with permission from [36]. Copyright 2017, Wiley-VCH.

3.1.3. Carbonised wood

In addition to coatings, another way to improve the absorption of light by wood is to convert it into a biochar by carbonisation, to make its surface darker and more porous. Indeed, during the pyrolysis of biomass with little or no oxygen, a biochar is formed. The process is highly scalable and the biochar can have a controlled pore size depending on the pyrolysis temperature, time, catalyst present during the process and activation after pyrolysis [47,48]. As shown in **Fig. 4**, carbonisation opens and develops the natural porosity of wood, which improves water transport. One way to achieve this is pyrolysis, which consists of treating the wood to a temperature of around 500 °C in the absence of oxygen to prevent its combustion, e.g. under nitrogen flow. This moderate temperature allows an intense darkening of the

surface without making the material hydrophobic, which would be detrimental to the desired capillary effect.

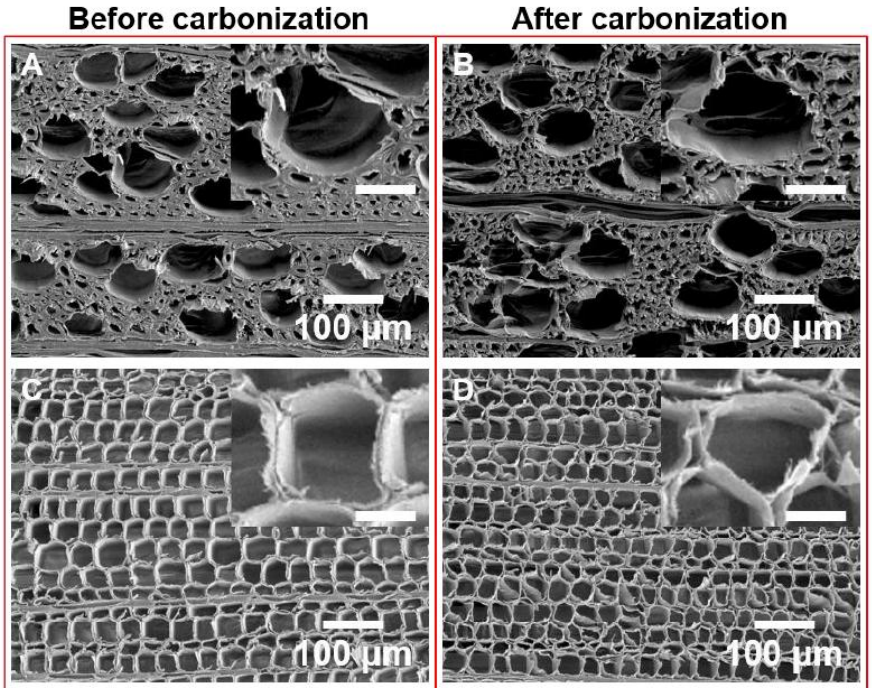

Fig. 4. SEM images of poplar (top) and pine (bottom) woods, before (left) and after (right) carbonisation. Reproduced from [41] Copyright (2017), with permission from Elsevier.

This process has been used in several studies, and its effectiveness ranges from 72% to 90% (see Table 1 in the next section). As shown in **Fig. 5**, the absorbance of the material is then much higher than that of natural wood. Another process is the use a laser to carbonise the surface of wood, which has the advantage of not damaging the pores and allows better control of the speed and accuracy of the process. However, with an evaporation rate of 2.52 kg m^{-2} h^{-1} under 3 suns (MERCP1: 0.84 kg m^{-2} h^{-1}), it gave poorer results than pyrolysis (2.88 kg m^{-2} h^{-1}, i.e., a MERCP1 of 0.96 kg m^{-2} h^{-1})) under the same test conditions [39]). The use of flames to treat the wood surface can also be considered but, like laser treatment, it did not show better efficacy than pyrolysis, with a water evaporation rate of 1.05 kg m^{-2} h^{-1} under 1 sun. It can be noted that the combination of pyrolysis and metallic coating is possible and can induce a higher evaporation rate. In fact, this is the method that has shown the best results of all the tests carried out [39]. By coating the wood with gold nanoparticles before carbonising it in a

second step, the surface structure is less degraded, less brittle, and therefore mechanically stronger and more durable.

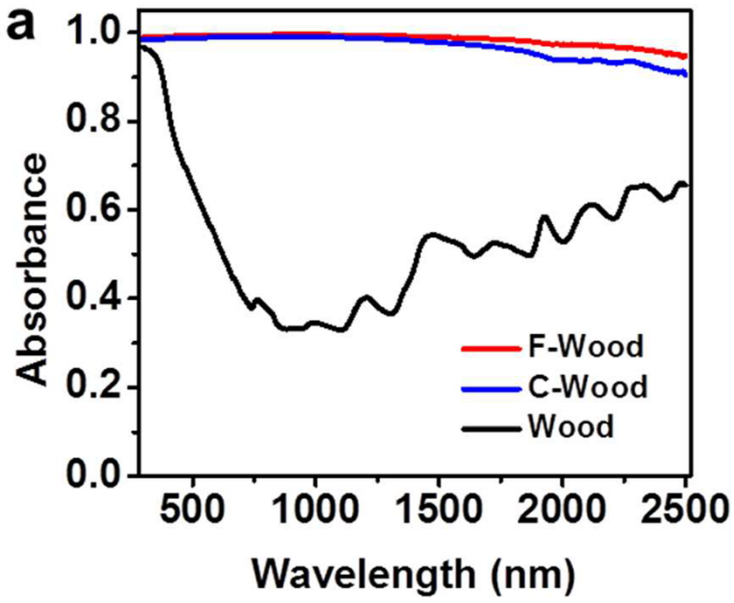

Fig. 5. Absorbance of flame-treated wood (F-Wood) and carbonised wood (C-Wood) compared to that of natural wood (Wood) as a function of wavelength. Reproduced with permission from [42]. Copyright (2017) American Chemical Society.

3.1.4. Other advantages of wood

Wood is not an isotropic material and therefore behaves differently parallel and perpendicular to the direction of the fibres. Some authors have shown the interest of cutting wood crosswise to study its radial porosity [40]. Wood has a lower thermal conductivity in the radial direction while its porosity is still high due to the connection between the inside and outside of the wood via the ligneous rays and lumens. Graphite has been sprayed at the surface of the wood sample to provide high photothermal properties. The result is an evaporation rate of 1.20 kg m^{-2} h^{-1} for an efficiency of 80%.

3.2. Annual plants and perennial plants

While wood has been well tested for the solar evaporation of water and gives good results, it is already used for its mechanical properties in the building industry, for the energy it

produces when burned, or to make furniture. All in all, it is a material that has a proven history of reliable service in many applications and which remains indispensable in the industry. Therefore, the exploration of less noble materials, which are poorly valorised or even considered as waste, can bring additional interest to solar evaporation. Rice straw, for instance, is often left and burned on site, which is a very polluting process [49]. It is therefore important to find a way to use this type of waste. The materials can also be used as such but after treatment to make their surface more light-absorbent, or in the form of biochar.

3.2.1. Plant stems

The first way non-wood plants have been tested as an evaporation system is in the form of bundles to transport water using their pipe geometry. The particular system used in the example shown in **Fig. 6** is based on *Juncus effusus*, a flowering herbaceous plant from China, coupled with sprayed carbon powder to give the light-absorption property and thus its dark appearance. The results of water evaporation under 1 sun were 2.23 $kg\ m^{-2}\ h^{-1}$, which is higher than usual and would give an efficiency of more than 100% using the regular enthalpy (equation (5)) for the energy supplied to the system. Indeed, the area used for evaporation is not only the top surface area but also the sides that are higher than the expandable polyethylene foam used as a float, allowing the system to favour evaporation in three dimensions (**Fig. 6**). This has been proven from results obtained with different heights of 0, 10 and 20 mm: the 20 mm system presented the best results. However, the reason why the height is important is that the structure of the *Juncus effusus* intrinsically has microscopic channels and when bundled together, the pipe geometry allows macroscopic spaces between each straw. These free spaces allow a higher area of solar evaporation, a longer optical path length, a lower thermal conductivity and the release of water vapour in several directions. Overall, the *Juncus effusus* system is very efficient [50].

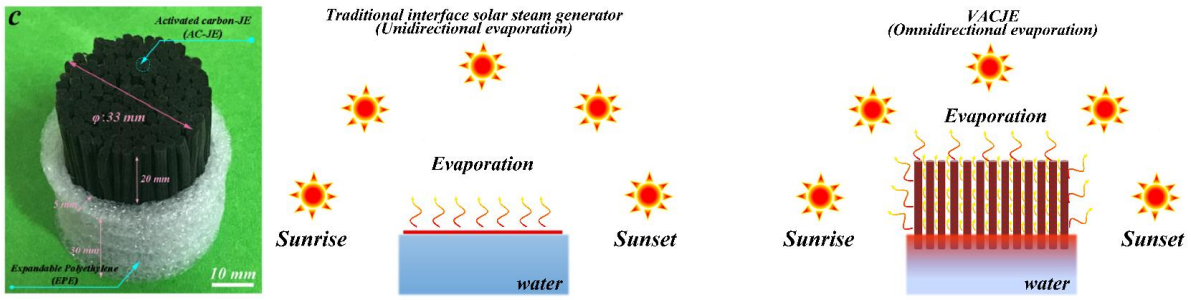

Fig. 6. Water evaporation system based on Juncus effusus (left) and its increased area available for a better solar absorption and evaporation (right), compared to a conventional interface solar steam generator (middle). Reproduced from [50]. Copyright (2020), with permission from Elsevier.

In addition to reeds, rice straws have been investigated for the same purpose. In contrast to the aforementioned system, this one used the upper leaves of the rice straw as absorbing material. To do this, the leaves were ground, packed and pyrolysed to form a flat surface that was then placed over the straws that serve as pipes to transport the water. While the former reeds, although surface-treated to better absorb light, were used directly as absorbing material, this system uses different parts of the plant to transport water and absorb light. However, this system based on rice by-products obtained medium results of 1.05 kg m^{-2} h^{-1} with an efficiency of 66% [37].

3.2.2. Vegetable "foams"

Another way to create a WES from straws is to make a vegetable foam-like material. Corn straws have been tested in this form in [51]. The straws were first microwaved for 90 seconds, then soaked in a 5 wt. % aqueous solution of KOH for 24 h. They were then washed with deionised water and freeze-dried to obtain a "foam". The treatment used to enhance light absorption was a layer of polypyrrole, a polymer known to absorb radiation in the near-infrared range. The resulting foam-like product is shown in **Fig. 7** and presents a remarkably low thermal conductivity of 0.027 W m^{-1} K^{-1}, indicating its excellent insulation properties, as

well as a wide range of pore sizes. The evaporation rate of water on corn straw "foam" was 1.77 kg m^{-2} h^{-1} under 1 sun irradiation, which represents an efficiency of 96%.

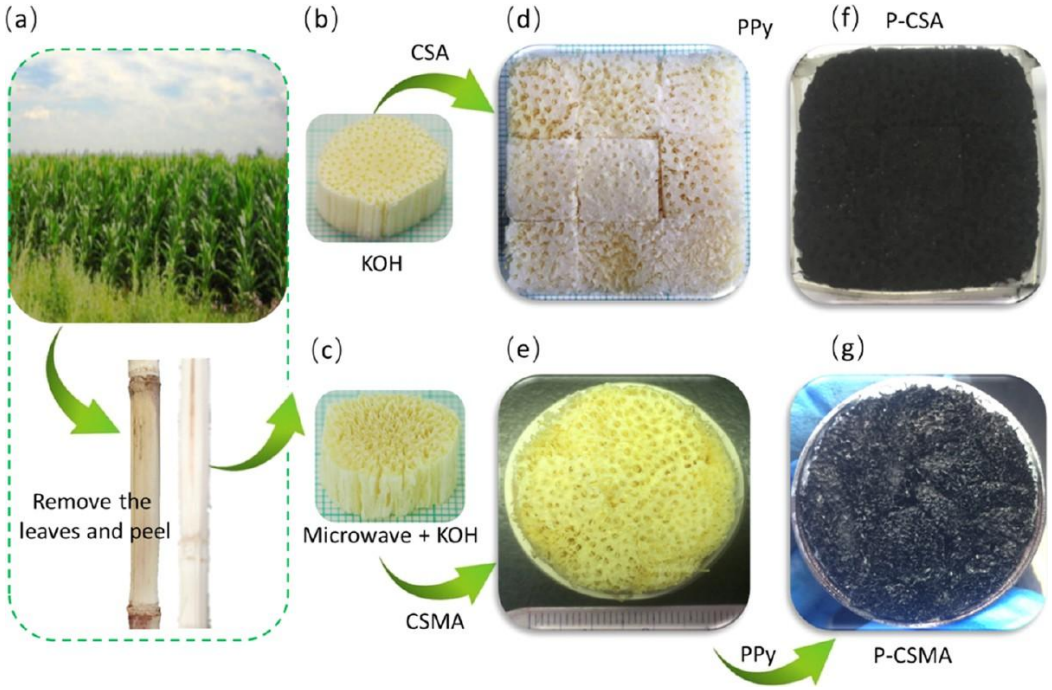

Fig. 7. Process of making a WES based on corn straw "foam". Reproduced with permission from [51]. Copyright (2020) American Chemical Society.

Foams are also an interesting technical solution for biomass waste that cannot be used because of its shape, such as rice husks [52]. As shown in **Fig. 8**, rice husk was first carbonised and then put in deionised water. A stirring process, which involved foaming agents and binders, was then used to produce a slurry. This slurry was then shaped into the desired form which, after freeze-drying, was porous and had a low thermal conductivity. To convert better light energy into heat, the rice "foam" was carbonised further. The resulting evaporation rate of the resultant biochar was 1.03 kg m^{-2} h^{-1} with an efficiency of 71%.

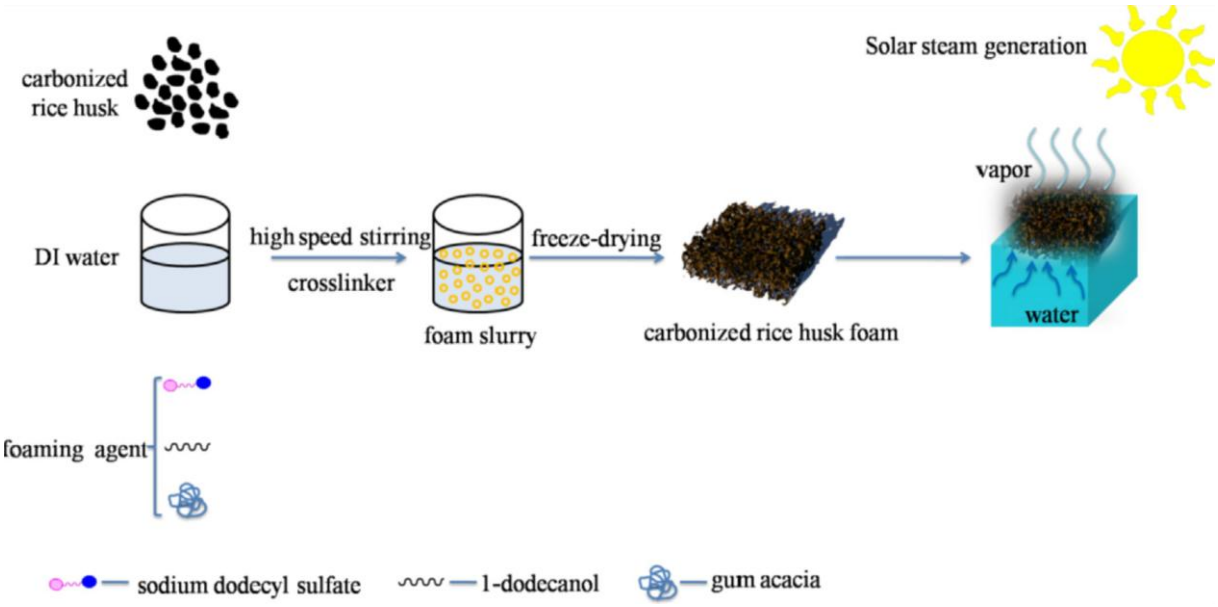

Fig. 8. Process of making a WES based on a foam-like material made of carbonised rice husk. Reproduced from [52]. Copyright (2020), with permission from Elsevier.

3.2.3. Lotus

Lotus is a plant for which interest has been found in solar evaporation. Two studies have used part of this plant to create a solar WES. On the one hand, the seedpod was used for its porous structure, which offers low thermal conductivity and high water absorption. Light absorption was improved by a pyrolysis process to achieve 98% to 99% over the wavelength range 250-2000 nm. In the end, when exposed to 1 sun irradiation, this system produced 1.30 kg m^{-2} h^{-1} with an efficiency of 87% [53].

On the other hand, lotus leaves were also tested [54]. Once carbonised (**Fig. 9**), their surface becomes hydrophilic and highly light-absorbent, making it a good surface to put on top of a water-transporting material. In the study, with a synthetic foam used as the transport material, the water evaporation rates doubled from 1.55 kg m^{-2} h^{-1} for bulk water to 3.10 kg m^{-2} h^{-1} using the system based on carbonised lotus leaf. During the experiment, the surface temperature was indeed much higher with the lotus system. This work thus confirms the interest of lotus leaves as biomass-based absorbing material.

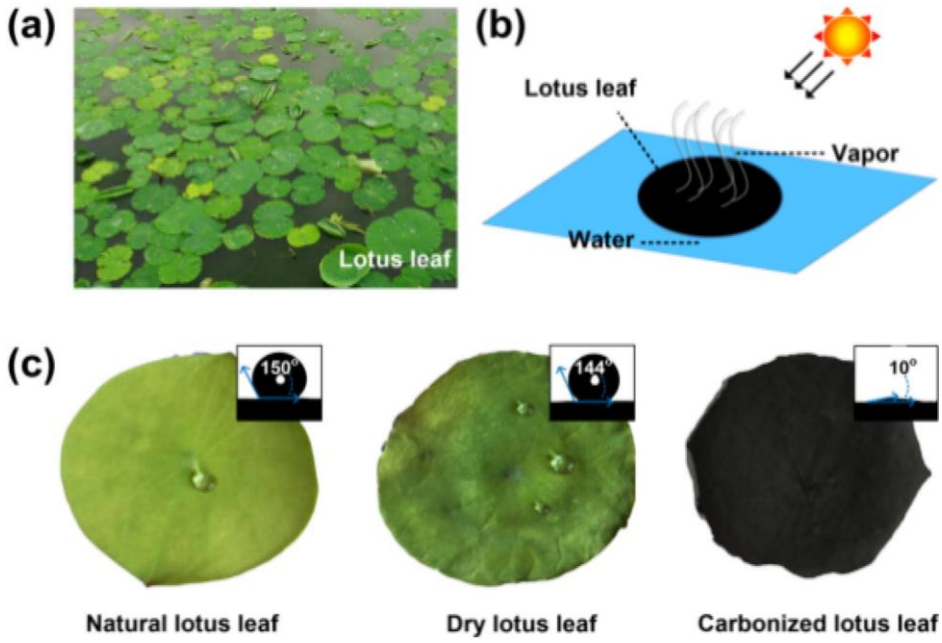

Fig. 9. (a) Lotus leaves found in nature, (b) process of evaporation via a carbonised lotus leaf, and (c) pictures of lotus leaf before drying, after drying and after carbonisation (from left to right), showing the changes of hydrophilic properties by the evolution of the water contact angle. Reproduced from [54]. Copyright (2019), with permission from Elsevier.

3.2.4. Bamboo

Bamboo is a grass plant with mechanical properties similar to those of wood. Its internodal spacing is hollow and the section presents a porous structure due to vessels. To make an evaporation device, Sheng et al. used several sections of different dimensions assembled to obtain a disc shape (**Fig. 10**) [55]. In addition to being a porous structure for water transport, bamboo also has a fairly low thermal conductivity, 0.30 W m^{-1} K^{-1}. To allow better photothermal properties, Sheng's team chose to deposit metallic nanoparticles such as Ag and Pd. The coated bamboo showed a high absorbance of 99% and in the end, this device was able to evaporate water at 12.3 kg m^{-2} h^{-1} under an irradiation corresponding to 10 suns (i.e., a MERCP1 of 1.23 kg m^{-2} h^{-1}) for an efficiency of 87%.

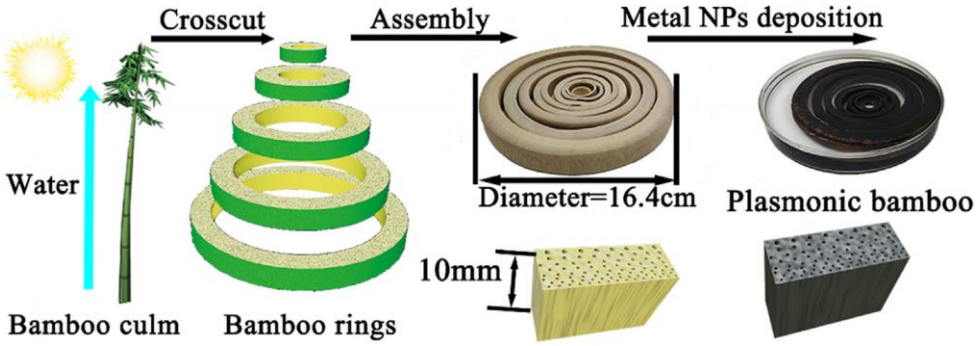

Fig. 10. Assembly of a bamboo-based WES. Reproduced from [55]. Copyright (2020), with permission from Elsevier.

3.3. Fruits and vegetables

3.3.1. Loofah

Loofah, a plant of the Cucurbitaceae family, is a sponge-like plant that has been used as a solar evaporation device in the form of biochar [56]. The process is illustrated in **Fig. 11** and involves a pre-treatment with ethanol and deionised water to clean the Loofah, followed by immersion in sodium hydroxide at 80 °C for 2 hours to remove the lignin. This was followed by pyrolysis under nitrogen at 500 °C. The result is a WES that produces 1.38 kg m^{-2} h^{-1} under 1 sun illumination, with 85% efficiency.

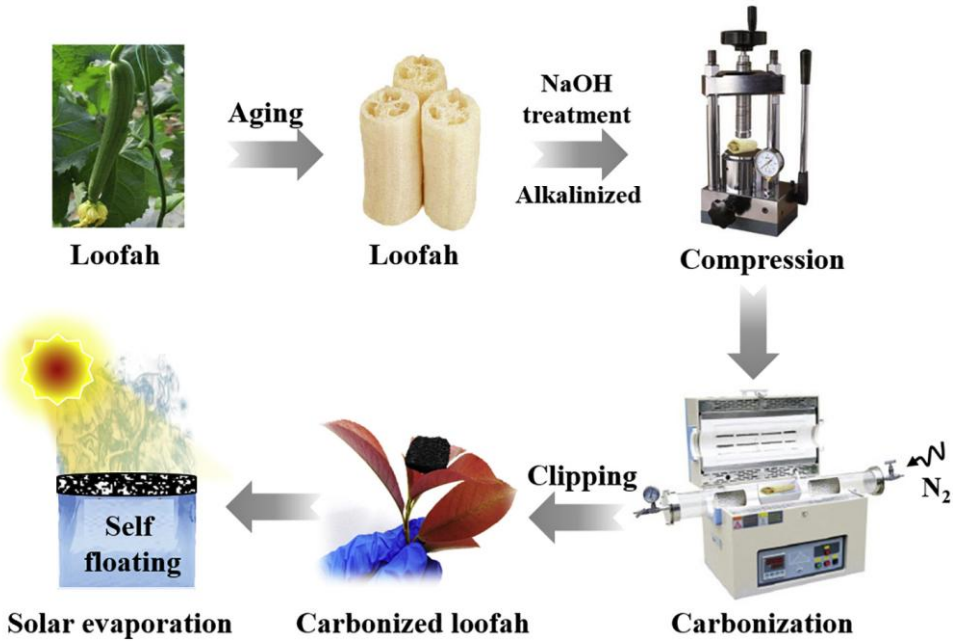

Fig. 11. Process to obtain a biochar from Loofah. Reproduced from [56]. Copyright (2020), with permission from Elsevier.

3.3.2. Radish

Radishes were cut vertically in the direction of growth and then carbonised at 500 °C [57]. The characterisation of the radish revealed a porous structure very similar to the vascular network of other plants already encountered in the examples in this review article, which ensures water transport to the surface and photon trapping, and the presence of surface chemical groups responsible for its hydrophilicity. In addition, the carbonised radish presented low density, low thermal conductivity and interesting photothermal properties. In short, the radish biochar has all the properties necessary for solar evaporation. The evaporation rate of carbonised radish was about 0.6 kg m^{-2} h^{-1} under 1 sun irradiation after subtracting natural evaporation in the dark, which is lower than that of other typical bio-based materials. To improve evaporation, two methods were used. First, the addition of an insulation layer under the carbonised radish improved the rate to 0.7 kg m^{-2} h^{-1} under the same conditions of irradiation. To further improve the evaporation, titanium nitride was used as an additional coating on the carbonised surface and the resulting evaporation rate reached 1.18 kg m^{-2} h^{-1} for an efficiency of 72% under 1 sun irradiation.

3.3.3. Carrot

Another material for solar evaporation that has been created from edible roots is carrot biochar [58]. The carrots were cut along the direction of growth with a thickness of about 1 cm. After being dehydrated in ethanol for 2 days and then dried, the slices were pyrolysed at 550 °C in argon for 30 min at a rate of 5 °C per minute. The carrot biochar presents a high light absorption of 84% (**Erreur ! Source du renvoi introuvable.**) and a hydrophilic surface. This biochar is able to produce 2.04 kg m^{-2} h^{-1} of water vapour with 127% efficiency (a value once more based on Equation (5), which here again shows its limitations). It can also be noted that the biochar retains its performance with a slight decrease in evaporation rate (0.24 kg m^{-2}

h^{-1}) for 4.7 hours after the light is turned off, showing that much of the energy is stored in the system.

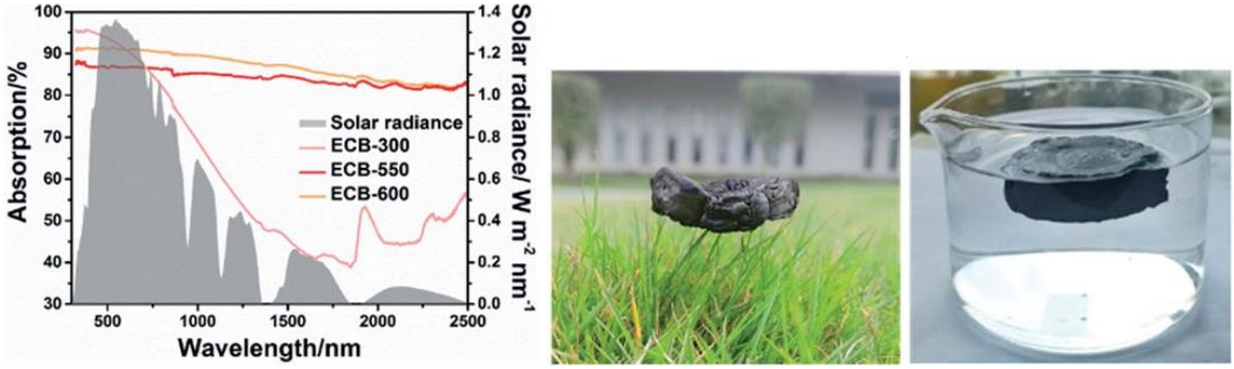

Fig. 12. A few characteristics of ethanol-treated-carrot biochar (ECB). From left to right: solar spectral irradiance (AM 1.5 G) (right axis) and absorption (left axis) of ECB at different pyrolysis temperatures (°C); lightness of ECB-550; the same material, floating on water. Reproduced with permission from [58]. Copyright (2019) The Royal Society of Chemistry.

3.3.4. Pomelo peel

Another atypical material suggested for solar evaporation is pomelo peel [59]. It is a food by-product that is usually discarded, making it a perfect material to avoid synthetic precursors for water transport. Besides, pomelo peel is thicker than usual vegetable peels, which makes it more compatible with evaporation. Polypyrrole was chosen as a means of improving light absorption, as it has already proven its capabilities and compatibility with bio-based materials. As shown is **Erreur ! Source du renvoi introuvable.**, the pomelo peel was first cut to the desired shape and then the yellow epidermis was removed as it is non-porous. It was then soaked in ethanol to clean the structure and make it more porous. A series of polymerisation processes followed to allow high photothermal properties using polypyrrole. The final product was then freeze-dried and the result was a WES material with over 95% absorption. In the same study, carbonised pomelo peel was also tested, which showed a more fragile structure, but capable of evaporating water at a rate of 1.09 kg m^{-2} h^{-1}. The freeze-dried polypyrrole-pomelo peel composite, however, reached 1.29 kg m^{-2} h^{-1}, which represents an efficiency of 80%.

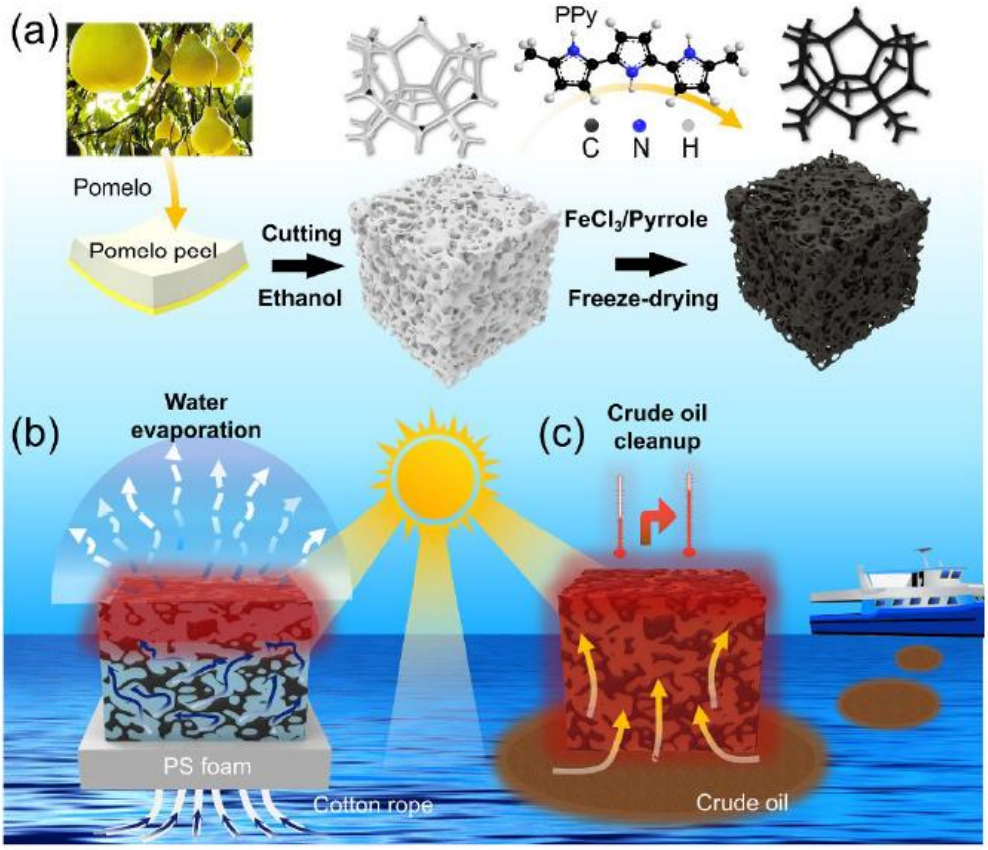

Fig. 13. (a) Process for the production of a porous material from pomelo peel. Possible applications of this material: (b) water solar evaporation or (c) treatment of oil spills. Reproduced with permission from [59]. Copyright (2020) American Chemical Society.

3.3.5. Mushroom

Species not yet mentioned are fungi. Some authors explored the abilities of a well-known mushroom, the shiitake mushroom, as the main component of an evaporation device [60]. Its shape with a large round surface for light absorption and its stipe for water transport make it a suitable candidate for WESs (**Erreur ! Source du renvoi introuvable.**). The mushroom was pyrolysed at 500 °C for 12h and the resulting dark surface was capable of absorbing about 96% of light. Hydrophilicity was present before and after carbonisation, as the surface functional groups remained the same. Combined with a porous structure, this resulted in a good capacity to transport water. This can be seen when evaporating without light, as the mushroom itself is capable of evaporating more than twice as much water as it would without it. This quantity is more than three times higher if the carbonised mushroom is used.

Furthermore, it is a relatively cheap product and carbonisation requires very little prior process, only soaking in water for softening the mushroom and cleaning it. The resulting water evaporation rate under 1 sun irradiation was 1.12 kg m^{-2} h^{-1} for the pristine mushroom and 1.48 kg m^{-2} h^{-1} for the pyrolysed mushroom, which means an efficiency of 62% and 78%, respectively.

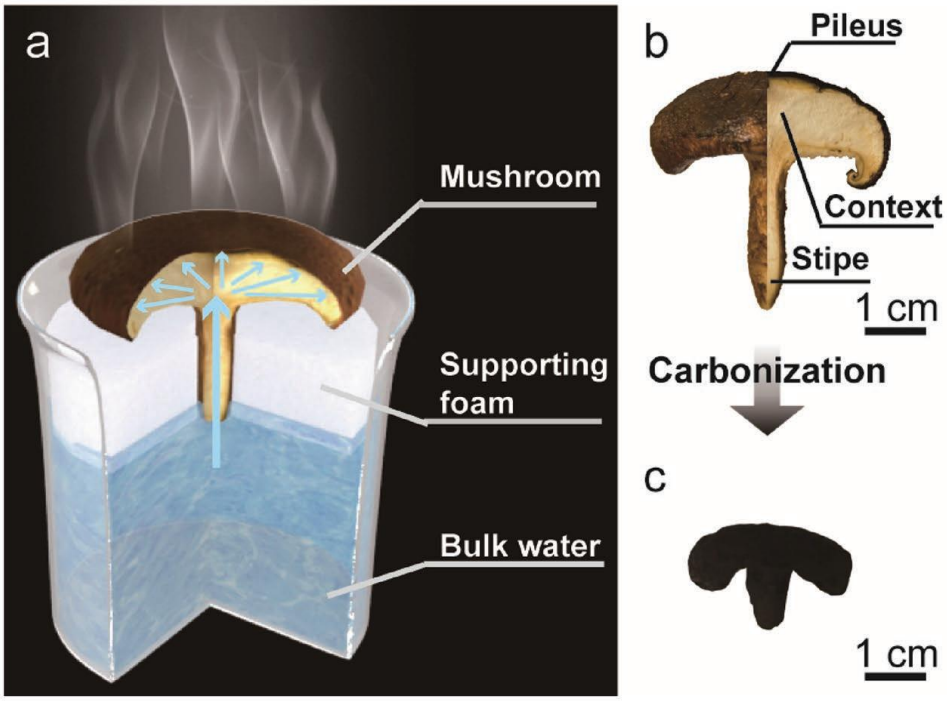

Fig. 14. (a) Mushroom-based WES device, and mushroom anatomy: (b) before and (c) after carbonisation. Reproduced with permission from [60]. Copyright 2017, Wiley-VCH.

3.4. Other natural or bio-inspired materials

Among the variety of living species available as precursors of materials for solar evaporation, some unusual biomasses have been investigated: willow catkins, miscellaneous plant wastes, algae or hollow carbon spheres that can be derived, for instance, from fish eggs. Living matter, whether plant or animal, has also inspired researchers to create more efficient evaporation systems as shown at the end of this section.

3.4.1. *Willow catkins*

Another plant derived biochar was created using willow catkins, a fluffy white blossom that floats in the air or lie on the ground in spring [61]. After being activated by a 2 mol L^{-1} KOH solution, the catkins were heated to 750 °C in a nitrogen environment at a rate of 5 °C per minute. The resulting carbonised catkins were then washed with HCl until the pH stabilised at 7. They were then added to a dopamine hydrochloride / Tris buffer solution, stirred for 8h and filtered. The resulting membrane was able to produce an ER of 1.65 kg m^{-2} h^{-1} with an efficiency of 90% under 1 sun illumination.

3.4.2. *Miscellaneous vegetable wastes*

Another biochar-based system has been proposed, but this time a variety of plant wastes were used (banana and orange peels, fallen leaves, branches and bamboo) [62]. All these wastes were carbonised and then crushed by hand and dissolved with ethylcellulose to obtain a slurry. This slurry was then deposited on filter paper to form the steam-generating device. This device had an evaporation rate of 1.21 kg m^{-2} h^{-1} with an efficiency of 80% while under 1 sun illumination.

3.4.3. *Algae*

Algae bloom is a rapid development of algae in a specific area due to a disturbance of the local ecosystem (fertiliser rejection, overfishing, etc.). The consequences on ecosystems and on human health are multiple, especially a local lack of oxygen due to algae or bacteria respiration during night or decomposition, respectively, strong odour and even potential disease transmissible through fish consumption [63]. Therefore, harvesting these algae for use may be a potential way to take advantage of this phenomenon while combating it.

The use of algae as water evaporation material makes sense because they live in water so that they have a hydrophilic porous structure that provides pathways for water transport, and

they can be carbonised. Yang et al. first tested several routes to utilise the green algae *Enteromorpha prolifera* [64]. The preparation processes are shown in **Fig. 15**. A first biochar was obtained by direct pyrolysis and deposited by spray-coating onto a cellulose acetate membrane. A second and a third biochar were made by orienting the algae in the direction of growth or perpendicularly, respectively, followed by pyrolysis. A fourth biochar was obtained after sonication, freeze-drying, and the resulting porous material, a cryogel, was pyrolysed. It is useful to note that carbonised algae are hydrophilic. Each of the resulting photothermal materials was placed on a polystyrene foam to act as a thermal barrier, equipped with a wick to transport water. In the end, the measured water evaporation rate increased from the 1st biochar to the 4th one, i.e., from SA1 to SA4 in **Fig. 15**. The most efficient material, SA4, led to an evaporation rate of 1.23 kg m^{-2} h^{-1} and an efficiency of 84% while the least performing, SA1, still reached 1.16 kg m^{-2} h^{-1} with an efficiency of 80%, thus demonstrating the relevance of the use of algae for solar water evaporation.

A similar study used the same algae to make a foam-like product, also supported on polystyrene foam wrapped in cotton to avoid heating the bulk of water and providing water to the surface. Results were best under a solar irradiation corresponding to 5 suns, with an evaporation rate of 7.09 kg m^{-2} h^{-1} (i.e., a MERCP1 of 1.42 kg m^{-2} h^{-1}) and an efficiency of 89% [65].

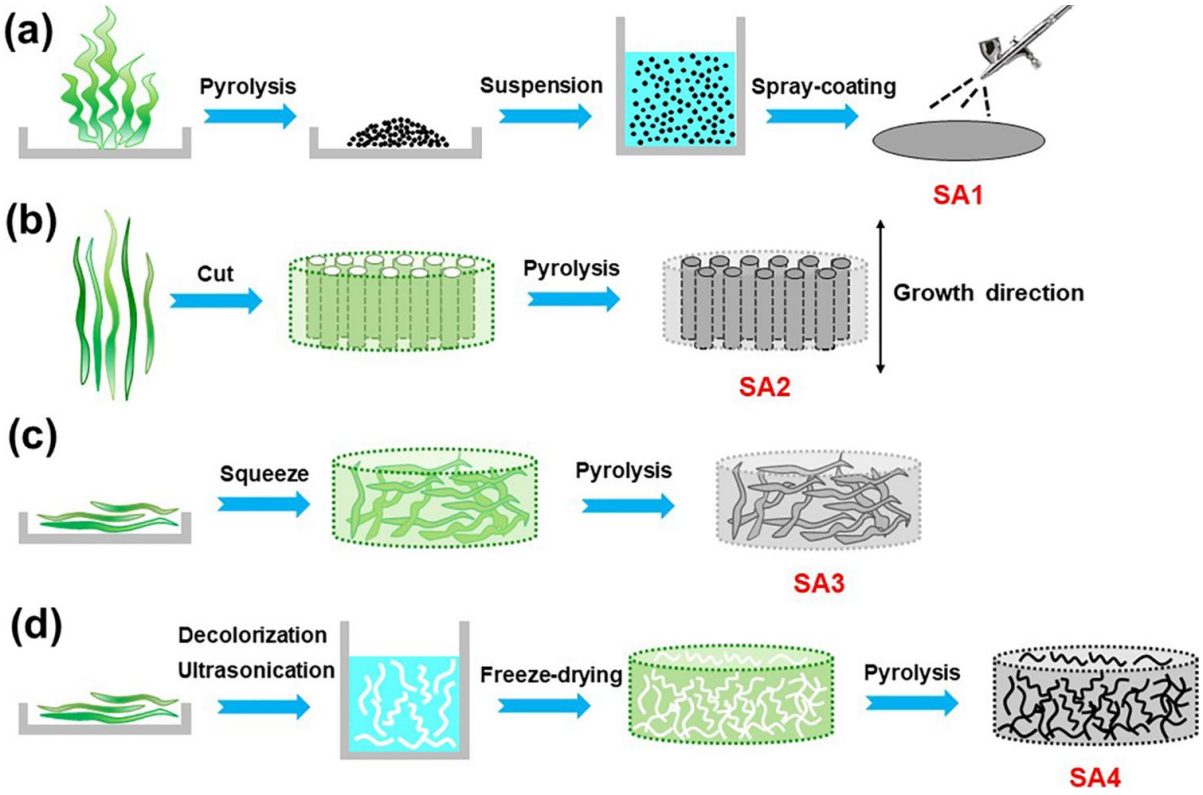

Fig. 15. Processes tested for producing WESs based on the Enteromorpha prolifera algae. Reproduced with permission from [64]. Copyright (2019) American Chemical Society.

Another study used green algae to create a superhydrophilic biochar [66]. Here, the pyrolysis was performed at 800 °C for 2h and the biochar was used without additional foam this time. Unlike the previous biochars presented in **Fig. 15**, which were hydrophilic, the present material initially had a water contact angle of 141°, meaning that it is hydrophobic. To make the surface of the biochar superhydrophilic, a photopolymerisation process of acrylic acid monomer was done at the surface, using benzophenone as a photo-initiator of the reaction. A water droplet placed on it was thus completely absorbed in 0.65 seconds. The product obtained is shown in **Fig. 16**. The evaporation rate achieved was 1.35 kg m^{-2} h^{-1} under 1 sun with an efficiency of 83%.

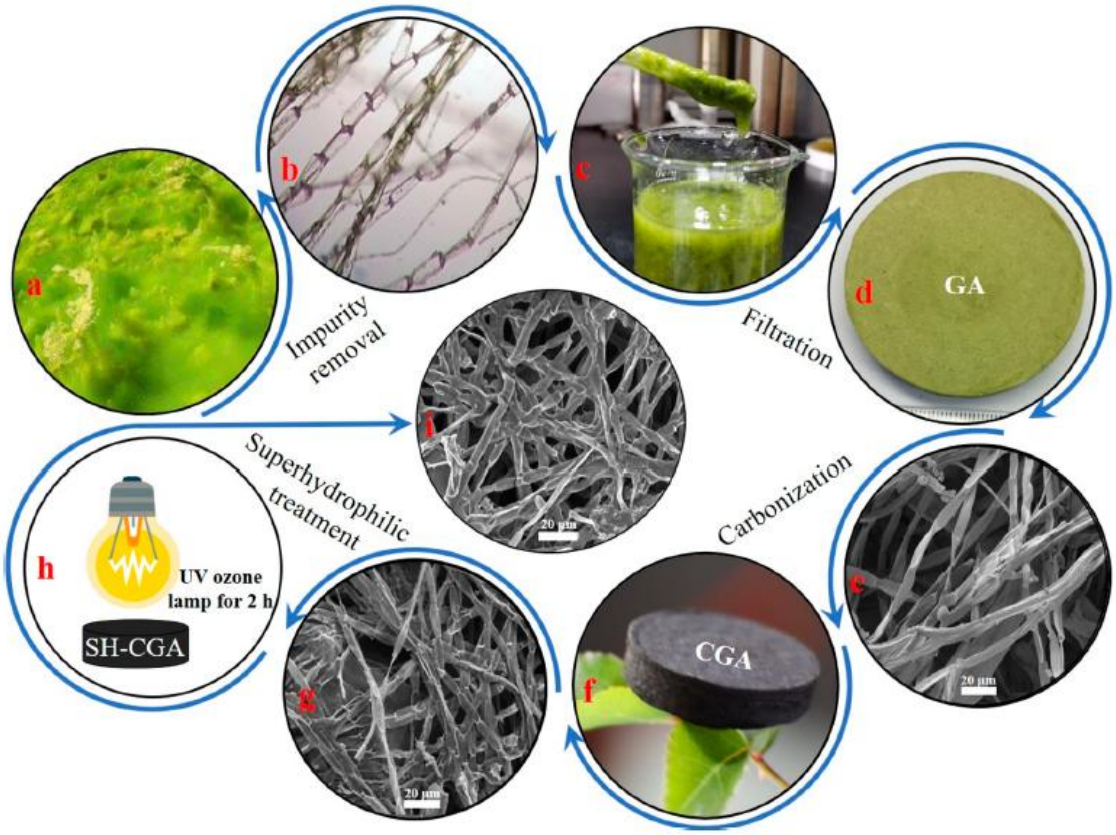

562

563 **Fig. 16.** Process to produce a WES based on superhydrophilic biochar derived from
564 carbonised algae. Reproduced with permission from [66]. Copyright (2020) American
565 Chemical Society.

566 *3.4.4. Hollow carbon spheres*

567 Hollow spheres are another type of material that can be used to improve the evaporation of
568 water under solar irradiation. Unlike most of the systems presented here, these spheres do not
569 require additional foam to float, precisely because they are hollow. In addition, the carbon
570 allows them to have good light absorption with low emissivity. A manufacturing process for
571 creating hollow carbon spheres is called hard-templating and is shown in **Fig. 17**. It consists
572 of coating the surface of a sacrificial spherical template with a carbonaceous precursor, for
573 example using a solution of monomers and various additives in an autoclave, to form a sphere
574 coated with hydrochar. The subsequent pyrolysis step eliminates the internal template and
575 converts the hydrochar surface layer into pure carbon. The result is a hollow carbon sphere.

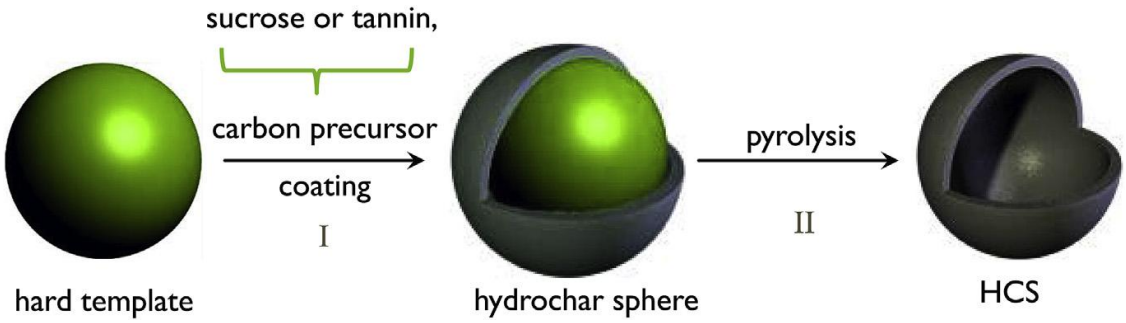

Fig. 17. Preparation scheme of hollow carbon spheres. Reproduced from [67]. Copyright (2019), with permission from Elsevier.

Hollow carbon spheres have been tested in [68] and reached 1.45 kg m^{-2} h^{-1} under an irradiation of 1 sun, which represents an efficiency of 63% taking into account the evaporation of water in the dark. Another recent study examined the effects of the size of the spheres, the nature of the carbon precursors used, the temperature at which the spheres are pyrolysed and the addition of metal salts to the solution used in the autoclave [67]. Using the biggest templates with sucrose as precursor, Fe^{3+} as graphitisation catalyst and a temperature of pyrolysis of 1500°C, the hollow carbon spheres presented an evaporation rate of 2.3 kg m^{-2} h^{-1} under 1 sun irradiation, for an efficiency of 80%.

While the precursors used (tannin and sugar, as shown in **Fig. 17**) are of biological origin, thus giving biosourced hollow carbon spheres, the templates used above were polymer beads. However, it is possible to use 100% bio-based materials to make such hollow carbon spheres by using commercial lumpfish eggs as templates [69].

3.4.5. Biomimetic materials

Although we do not know of any concrete examples where nature is directly used for solar evaporation, it can nevertheless be a source of inspiration for creating new materials. For example, the water lily was used by Xu et al. to create a device that reproduces its behaviour on water [70]. This bio-inspired system has three layers: a solar absorber at the top, a support layer at the bottom to float on the water, and a water chamber inside. This structure has been reproduced with a Cu-based solar absorber that rests on a polystyrene foam in such a way that

598 there is a gap between the two. The foam at the bottom has holes that allow water to fill this
599 gap. The measured evaporation rate was 1.27 kg m^{-2} h^{-1} under 1 sun irradiation, for an
600 efficiency of 77%.

601 Another study uses the liquid transportation properties of the asymmetric capillary ratchet
602 of the bird beak and the pitcher plant peristome surface [32]. It is carried out by 3D printing of
603 a resin loaded with sodium citrate particles that are removed after solidification to produce
604 micropores. CNTs form the photothermal layer, which allows more than 90% of the light to
605 be absorbed. The resulting evaporation rate under 1 sun illumination is 2.63 kg m^{-2} h^{-1} for an
606 efficiency of 96%.

607 ***3.5. Gels***

608 Among the multitude of systems tested for solar evaporation, the most effective so far are
609 those based on gel. Gels, generally referred to as hydrogels or xero-/cryo-/aero-gels
610 depending on whether they are hydrated or have been dried by different methods, respectively
611 [71–73], are sponge-like or very light materials, respectively, which have a hydrophilic
612 porous structure and a low thermal conductivity. Hydrogels are the current leading materials
613 for solar water evaporation, as their evaporation rates are the highest. For example, under one
614 sun irradiation, a hydrogel based on polyvinyl alcohol (PVA) coupled with titanium
615 sesquioxide nanoparticles to absorb light achieved 3.6 kg m^{-2} h^{-1} for an efficiency of 90%
616 [74]. A PVA hydrogel coupled with polypyrrole achieved similar results of 3.6 kg m^{-2} h^{-1} for
617 an efficiency of 92% under the same conditions of irradiation [75]. Most gels thus typically
618 include PVA and a photothermal material to give them broadband light absorption properties.
619 This can be achieved through the use of metallic nanoparticles, graphene or polypyrrole, but
620 as the latter materials are generally expensive, biomass-based approaches such as those
621 suggested below should be preferred [76,77].

3.5.1. Aerogels

As mentioned before, algae in different forms have been tested. One of them, the fourth material (SA4) in **Fig. 16**, was a cryogel (abusively called "aerogel" whereas it has not been dried in supercritical conditions) that achieved an evaporation rate of 1.23 kg m^{-2} h^{-1} with an efficiency of 84% [64]. Another cryogel (also improperly called aerogel for the same reason) was produced from cellulose extracted from rice straw in the presence of reduced graphene oxide used as photothermal material and sodium alginate used as strengthening agent [77]. The result is a material with a porous structure that can absorb 20 times its weight in water, allowing it to continue producing steam long after it has been removed from water. It therefore behaves like a sponge that does not need a continuous supply of water. An evaporation rate of 2.25 kg m^{-2} h^{-1} has been measured, with 30% of this water evaporating without any light energy, leading to a net ER of 1.29 kg m^{-2} h^{-1}, which gives an efficiency of 89%. This means that a significant amount of energy is taken from the environment, allowing a higher evaporation rate than usual.

Another system, shown in **Fig. 18**, used bacterial nanocellulose and reduced graphene oxide to form a hydrogel [78]. Reduced graphene oxide was added during the growth of *Gluconacetobacter hansenii* bacteria to form a hydrogel, which was then cleaned and freeze-dried. The resulting cryogel (again referred to as aerogel in the original paper) then had a two-layer structure, one (top) layer having photothermal evaporation capabilities and the other (bottom) layer being adapted for water transport. This cryogel was only tested under the equivalent of 10 suns, which gave an evaporation rate of 11.8 kg m^{-2} h^{-1} (i.e., a MERCP1 of 1.18 kg m^{-2} h^{-1}) for an efficiency of 83%.

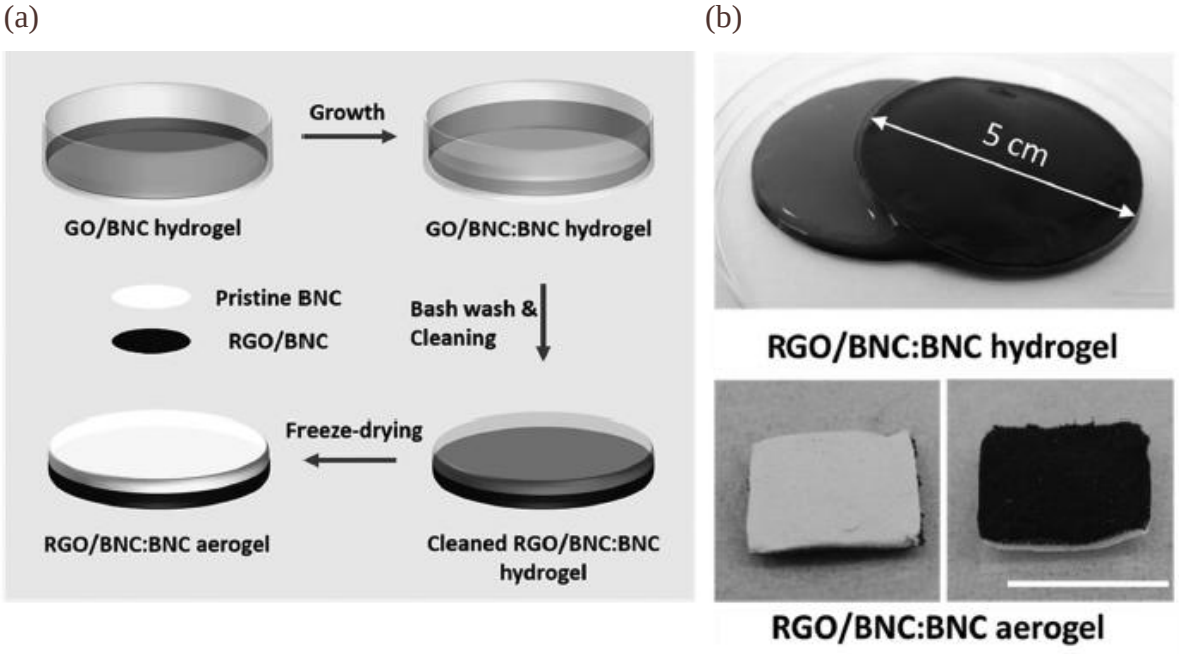

Fig. 18. (a) Process for the manufacture of bacterial nanocellulose (BNC)-based hydrogel and aerogel; (b) photographs of the corresponding materials. Reproduced with permission from [78]. Copyright 2016, Wiley-VCH.

Another unusual type of material found in nature is attapulgite clay. Although it is not bio-based, it is a natural material so it is worth mentioning in the present review. In fact, the WES made from this clay is based on an attapulgite – polymer composite, and this polymer could also just as well be of bio-based origin. Jia et al. [79] therefore used this clay to produce a two-layer composite. To do this, they first prepared an attapulgite – polyacrylamide composite and then applied flame treatment with a butane torch. The surface of the resulting lightweight two-layer composite (shown in **Fig. 19**) had a high light absorption of 99%, and the composite structure had a porosity similar to that of attapulgite clay, which provides sufficient pathways for the transport of water. Moreover, the thermal conductivity was 0.07 W m^{-1} K^{-1}, which is excellent for insulating the bulk water from incident energy. The resulting evaporation rate was 1.2 kg m^{-2} h^{-1}, which represents an efficiency of 85%.

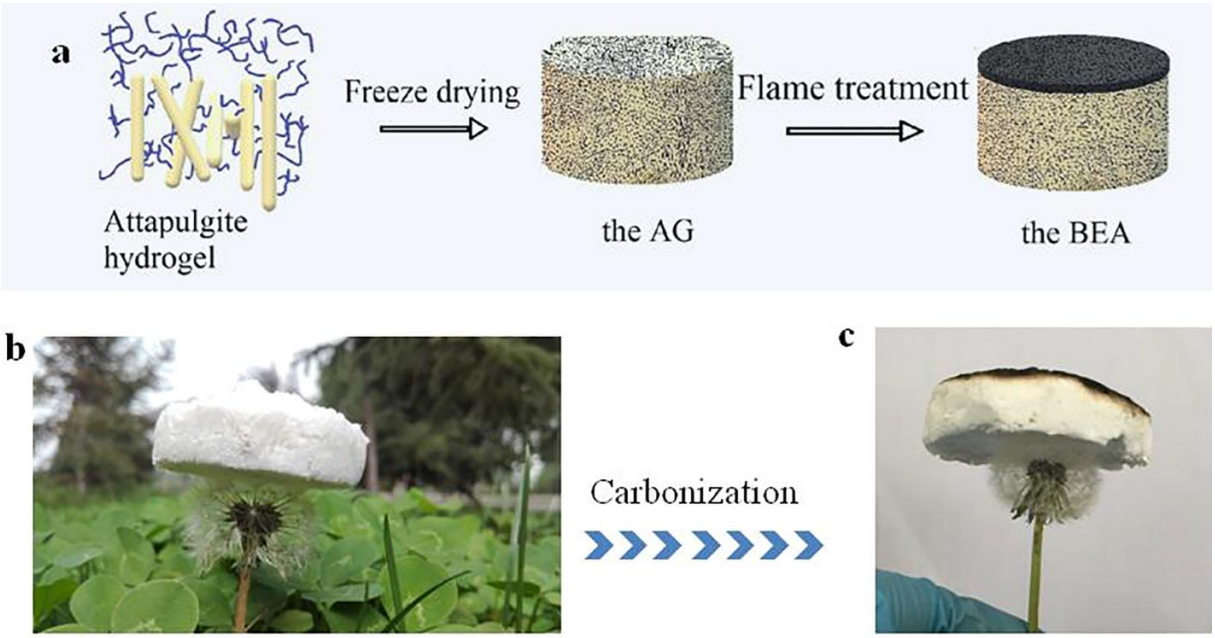

Fig. 19. (a) Process of making a two-layer attapulgite – polyacrylamide composite; (b) the same composite on a dandelion before (b) and after (c) carbonisation of the upper surface. Reproduced from [79]. Copyright (2019), with permission from Elsevier.

3.5.2. Hydrogels

As mentioned at the beginning of section 3.5, the most efficient gels are hydrogels [33,74,75]. To date, only one study has reported a biomaterial used to prepare a hydrogel that can be used as WES, while other studies generally use hydrogels as precursors to make aerogels. The biomass-based hydrogel was made from glucomannan, a hemicellulose component in the cell walls of the *konjac* plant (*Amorphophallus konjac*), coupled with carbonised metal-organic frameworks nanoparticles as the solar absorbing additive and polyvinyl alcohol [76]. The water evaporation rate was 3.2 kg m^{-2} h^{-1} with an efficiency of 90%. This rate is more than twice the average of all other systems. This is due to polyvinyl alcohol which is highly hydrophilic and, as the main polymeric molecular mesh, is capable of lowering the enthalpy of evaporation of water [3]. Water molecules indeed interact with fewer of their close neighbours through hydrogen bonds. Hydrogels have polar functional groups that can bind stronger with water molecules than the water molecules themselves [3].

Category	Type	Evaporation	Irradiation	MERCP1	Efficiency	Reference

4. Discussion

4.1. Performance of natural materials for solar evaporation

Biomass has a very great potential because there are many ways to allow it to be the basis of efficient evaporation systems while being a natural product with little or no value, and possibly even a waste product, such as straw that is usually burned, which is harmful to the environment, or the algae that swarm the coasts every year.

Table 1 lists most of the devices previously discussed category by category. Two categories are dedicated to wood, as the number of studies is higher relative to other biomass products. The first deals with carbonised wood, a category based only on transformation processes without the use of foreign materials, while the second deals with coatings based on metallic particles, among other things. The third category includes all other types of natural (mainly biomass) products, such as non-wood plants, algae, and other more atypical raw materials. It should be noticed that most of the materials in this category are biochars. The fourth and last category is dedicated to gels.

The efficiency ranges from 53% for the laser-treated wood to 96% for the corn straw foam. As previously said, this number alone does not express the level of performance of the system. For this reason, the hybrid gel based on *konjac* plant of [76] shows only 90% efficiency while evaporating almost twice as much water as corn straw foam of [51] that has 96% efficiency. Overall, carbonised wood subjected to 1 sun irradiation gives slightly lower results than coated wood, with the exception of a few results at a higher solar intensity, for which it has an efficiency greater than 80%. However, other carbonised biomass products, such as the lotus seedpod, algae biochar and algae foam perform fairly well when carbonised.

		rate (kg m^{-2} h^{-1})	(kW m^{-2})	(kg m^{-2} h^{-1})		
Carbonised wood	Basswood with drilled holes	1.04	1	1.04	75%	[80]
	Flames-treated basswood	1.05	1	1.05	72%	[42]
	Balsa wood	1.17	1	1.17	61%*	[81]
	Poplar with laser treatment	2.52	3	0.84	53%	[39]
	Wood	6.89	5	1.38	87%	[82]
	Flexible balsa & carbon nanotubes	11.22	10	1.12	81%	[19]
	Poplar	12.10	10	1.21	87%	[41]
	Basswood	12.20	10	1.22	90%	[83]
Coated wood	Basswood & $CuFeSe_2$ nanoparticles	1.20	1	1.20	68%	[45]
	Crosswise basswood & graphite	1.20	1	1.20	80%	[40]
	Basswood & tungsten trioxide	1.28	1	1.28	83%	[46]
	Pine wood & polydopamine	1.38	1	1.38	87%	[36]
	Poplar & tannic acid – Fe^{3+} complexes	1.85	1	1.85	90%	[38]
	Poplar & heat treatment and Au nanoparticles	4.02	3	1.34	84%	[39]
	Pine wood & polydopamine	7.54	3.5	2.15	135%	[36]
	Basswood & Pd nano particles	11.80	10	1.18	85%	[29]
	Basswood & graphene	14.02	12	1.17	83%	[84]
Other products based on natural or bio-inspired materials	Rice husk carbon foam	1.03	1	1.03	71%	[52]
	Rice straw	1.05	1	1.05	66%	[37]
	Radish biochar	1.18	1	1.18	72%	[57]
	Plant waste biochar	1.21	1	1.21	80%	[62]
	Algae biochar	1.21	1	1.21	83%	[64]
	Pomelo peel & polypyrrole	1.22	1	1.22	80%	[59]
	Water lily-inspired WES	1.27	1	1.27	77%	[70]
	Lotus seedpod biochar	1.30	1	1.30	87%	[53]
	Algae biochar	1.35	1	1.35	83%	[66]
	Loofah biochar	1.38	1	1.38	85%	[56]
	Hollow carbon spheres	1.45	1	1.45	63%	[68]
	Mushroom biochar	1.48	1	1.48	78%	[60]
	Willow catkin biochar	1.65	1	1.65	90%	[61]
	Corn straw foam	1.77	1	1.77	96%	[51]
	Carrot biochar	2.04	1	2.04	127%*	[58]
	Improved hollow carbon spheres	2.3	1	2.3	80%	[67]
	Juncus effusus fibrils	2.23	1	2.25	124%*	[50]
	Biomimetic 3D-printed structure	2.63	1	2.63	96%	[32]
	Lotus leaves	3.10	3**	1.03	74%*	[54]
	Algae carbon foam	7.09	5	1.42	89%	[65]
	Bamboo & plasmonic particles	12.80	10	1.28	87%	[55]

Gels	Attapulgite & poly acrylamide	1.20	1	1.20	85%	[79]
	Algae aerogel	1.23	1	1.23	84%	[64]
	Rice straw aerogel	2.25	1	2.25	89%	[77]
	Konjac glucomannan hybrid gel	3.20	1	3.20	90%	[76]
	Bacterial cellulose hydrogel	11.80	10	1.18	83%	[78]

Table 1. Natural materials for WESs reported in this review.

* Not mentioned in the original reference but calculated using Equation (5) with the enthalpy equation of [85].
** Not mentioned in the original reference but deduced from the evaporation rate.

Some promising results stand out. These include pine wood with polydopamine which, under 3.5 sun irradiation, is so efficient that the top layer of water boils and bubbles form and burst. The authors hypothesised that when bubbles burst, the water near them "perspires" into the air, which reduces the average energy required for evaporation [36]. Another remarkable result is obtained with the *Juncus effusus* fibril device, which allows larger than usual amounts of water to be evaporated due to its omnidirectional evaporation. Moreover, the hybrid gel based on konjac plant [76] is, as previously mentioned, the system that evaporates the most water under 1 sun irradiation and is close to the best hydrogels based on PVA achieved to date [74,75].

4.2. Ways to increase performance

All these biomasses, with the few exceptions mentioned above, finally give rather similar results, and this is quite normal since the porous structures are generally not very different from each other and their chemical composition is also quite alike. So the only way to really increase performance is, as we have seen, to:

- Modify the surfaces by more or less complex treatments to darken the top of the materials or to give them particular photothermal properties;

- Build systems from more suitable materials than biomass, which had proven to be economically and environmentally interesting, but in a bio-inspired way. In this case, biomass as such is no longer essential for itself, but it can be used as a source of inspiration to

implement resources that are not necessarily natural, as long as they prove to be more efficient.

- Solve the problems of fouling and clogging by impurities and salts, which deserve attention when the sustainability of performance and the life span of evaporation systems are considered. Indeed, in addition to the efficiency of evaporation alone, recent studies have begun to consider the longevity of the systems studied for seawater evaporation [14,24,65]. Given the salinity of seawater (3.5 wt.%), salt crystals form and tend to clog the pores necessary for water transport and settle on the surface where evaporation takes place, making the system less and less efficient. Two studies have been carried out on balsa wood. Zhang et al. showed degradation by evaporation of seawater over several days and even hours when evaporating Dead Sea water, which has a salt concentration of 27 wt.% [81]. On the contrary, He et al. have shown that the efficiency remains constant for this material after 7 hours at 15% salinity under 6 suns [86]. The authors explained it by the bimodal structure distributed in small pores allowing the transfer of water by capillarity to the surface, and in larger pores allowing the evacuation of water with a high salt content to the bottom. These two studies highlight the importance of the salinity level in comparing studies with each other. Based on the previous observation of a hierarchical network of pores, one of the solutions developed for wood was to drill holes, as shown in **Fig. 20**(a). This method gives a very stable evaporation rate over 100 h [80] for a salinity range of up to 20 wt.%.

On the same principle, bamboo has open channels that give it self-cleaning capabilities with an efficiency of 87% at 3.1% salinity [55]. This also applies to corn straws [51], with an efficiency of 94% at 20% salinity, which is remarkable because it does not require any additional design. Basswood, on the other hand, has a self-cleaning capacity after exposure to sunlight [29].

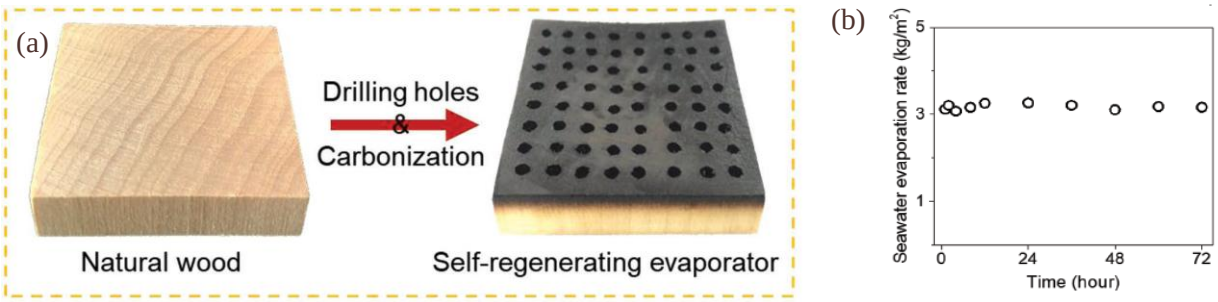

Fig. 20. (a) Method to avoid the effects of salt in a WES using seawater. Reproduced with permission from [80]. Copyright 2019, Wiley-VCH. (b) Rate of solar evaporation of seawater over time, using a *konjac* glucomannan hybrid gel. Reproduced with permission from [76]. Copyright 2020, Wiley-VCH.

Hydrogels have been shown to be able to self-clean effectively through the diffusion and discharge of salt ions into the brine. The hydrogel developed by Zhou et al. showed no trace of crystallisation after 12 hours of testing for salinities between 5 and 20%, in contrast to a salinity of 25% where crystallisation was observed on the material, which greatly degraded the evaporation performance [11]. The performance of hydrogels does not degrade over time for unsaturated salt solutions (< 25 wt.%), which was confirmed by Guo et al. [76] (**Fig. 20**(b)).

The water lily–inspired hierarchical design developed by Xu et al. is very interesting thanks to the complete separation between salt and water. Indeed, when the water is completely evaporated, the salt is stored under the WES with a constant WER throughout the process [70]. The concept of this system is to create a thin layer of water sandwiched between the upper hydrophobic absorber and the lower support that prevents crystallisation on the surface.

Another method was used to mitigate the effect of salt crystals in a layer around the WES by using the principle of the coffee-ring effect and the law of crystal nucleus growth [66]. Cotton threads are placed on the rim of the container and when the NaCl solution soaks in cotton, it causes the salt to crystallise after evaporation. The advantage is that the layers of

crystallised salt grow outside the evaporation system, so that the latter is not clogged and the liquid phase is separated from the salt (**Fig. 20**).

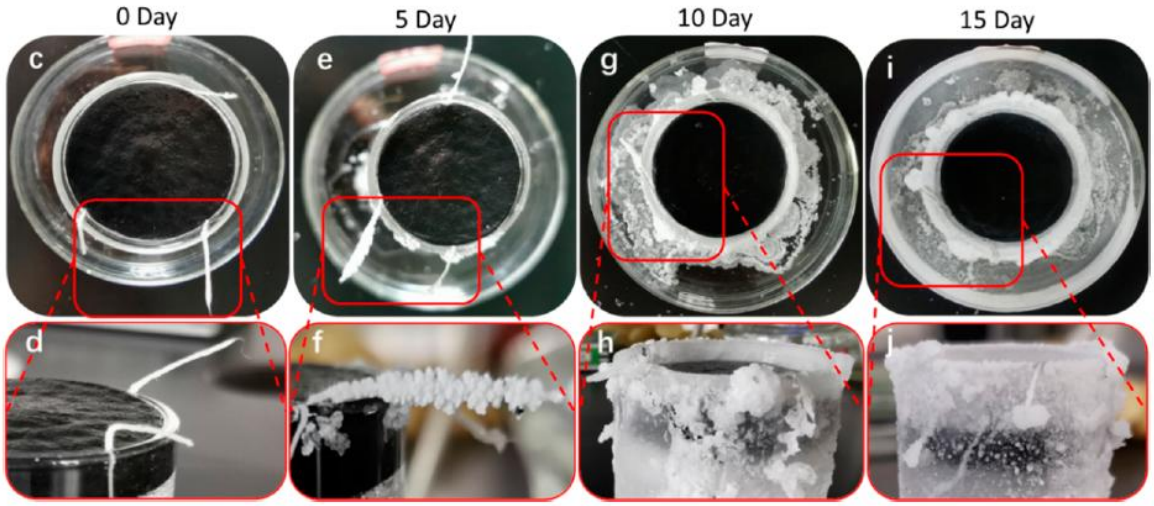

Fig. 21. Photos showing the progressive rejection of salt rejection from an evaporation structure based on superhydrophilic carbonised green algae, around which cotton threads were installed [66]. Copyright 2020, American Chemical Society.

Wu et al. also used a salt crystallisation strategy outside the WES. To do this, thanks to the design bio-inspired by a bird's beak by 3D printing, their conical system allows the salt to crystallise at the top, allowing easy extraction of the crystals [32]. The system has a high evaporation rate with an efficiency of more than 96% at 25% of salinity (**Fig. 20**).

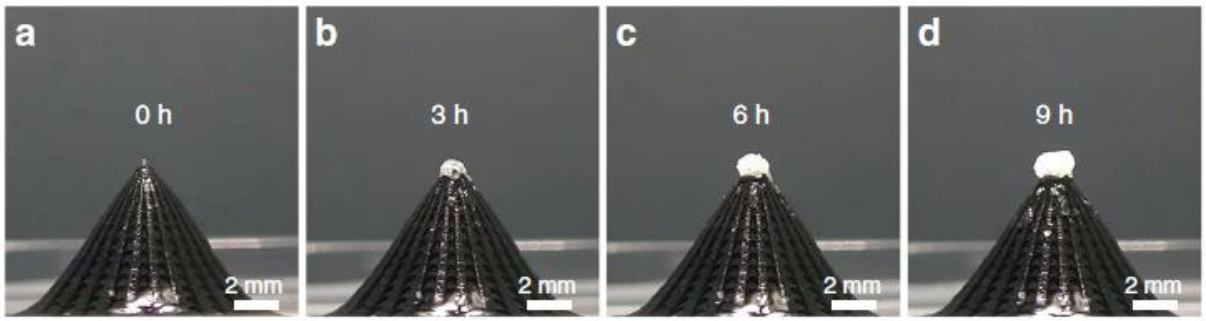

Fig. 22. Time sequence of photos showing the localized crystallisation process at the top of a biomimetic 3D evaporator inspired by birds' beaks [32]. Copyright 2020, Nature Communications.

Finally, some studies have tested materials outdoors, i.e., under real conditions. Surprisingly, the pine wood – polydopamine composite was found to be much more effective under 1.04 sun outdoors than under 1 sun in a controlled environment. The evaporation rate under real sunlight was indeed 2.13 kg m^{-2} h^{-1}, i.e., higher by 0.70 kg m^{-2} h^{-1} than in the lab [36]. The WES made from rice straw gave about 0.75 kg m^{-2} h^{-1} during sunny days of 9.5 h under 0.8 to 0.9 sun (based on the original article measurements) [37]. Finally, the algae-based biochar produced 0.95 kg m^{-2} h^{-1} under 0.8 sun (MERCP1 = 1.18 kg m^{-2} h^{-1}) [64].

5. Conclusion

In this review, the existing variety of solar water evaporation systems based on biomass and other natural products was reviewed. At present, wood has been tested from different perspectives, from carbonising or coating to give it better photothermal properties, to drilling holes to improve its durability in use, or cutting it perpendicularly to the longitudinal direction to use its anisotropy as an advantage. Various plants have also been investigated in different forms. First of all, their original shape allows them to be used as pipes for the stems, as photothermal surfaces for the leaves, or in the form of foam due to their natural porosity. Algae have also been used as a material for water evaporation devices, in the form of biochar or even aerogel. Indeed, gels can be prepared from materials of natural origin, in order to reduce their cost and environmental impact with respect to synthetic ones. Even more atypical materials have been explored, such as food waste, fungi or clay. Finally, biomimicry also appears to be a promising way to significantly improve the performance of solar evaporation systems, even if in this case nature is no longer used as a resource but as a model. This approach is particularly effective in increasing the longevity of the WESs, especially in the presence of salt.

Overall, water evaporation systems based on natural materials, and in particular on biomass, are more than capable of meeting the need for clean water production with efficient conversion of solar radiation without the need of an additional energy source. However, as some works have already shown, durability must be taken into account, as it can seriously affect the efficiency over a few cycles. This is particularly the case when using these devices to remove traces of oil or soil contaminants from the water, or when desalinating seawater, as pollutants or salt can quickly clog up the systems. Durability is therefore a necessary criterion when studying a material for solar evaporation and must be taken into account in future studies. In addition, further investigation and modelling of the interaction of water within materials will allow for more alternative ways to achieve higher evaporation rates.

Acknowledgement

This study was supported by the TALiSMAN project, funded by ERDF (2019-000214).

References

[1] N.S. Lewis, D.G. Nocera, Powering the planet: Chemical challenges in solar energy utilization, Proc. Natl. Acad. Sci. U. S. A. 103 (2006) 15729–15735. https://doi.org/10.1073/pnas.0603395103.

[2] P. Zhang, Q. Liao, H. Yao, Y. Huang, H. Cheng, L. Qu, Direct solar steam generation system for clean water production, Energy Storage Mater. 18 (2019) 429–446. https://doi.org/10.1016/j.ensm.2018.10.006.

[3] F. Zhao, Y. Guo, X. Zhou, W. Shi, G. Yu, Materials for solar-powered water evaporation, Nat. Rev. Mater. (2020) 1–14. https://doi.org/10.1038/s41578-020-0182-4.

[4] S. Chu, A. Majumdar, Opportunities and challenges for a sustainable energy future, Nature. 488 (2012) 294–303. https://doi.org/10.1038/nature11475.

[5] M. Gao, L. Zhu, C.K. Peh, G.W. Ho, Solar absorber material and system designs for photothermal water vaporization towards clean water and energy production, Energy Environ. Sci. 12 (2019) 841–864. https://doi.org/10.1039/C8EE01146J.

[6] K. Bae, G. Kang, S.K. Cho, W. Park, K. Kim, W.J. Padilla, Flexible thin-film black gold membranes with ultrabroadband plasmonic nanofocusing for efficient solar vapour generation, Nat. Commun. 6 (2015) 10103. https://doi.org/10.1038/ncomms10103.

[7] J. Wang, Y. Li, L. Deng, N. Wei, Y. Weng, S. Dong, D. Qi, J. Qiu, X. Chen, T. Wu, High-Performance Photothermal Conversion of Narrow-Bandgap Ti2O3 Nanoparticles, Adv. Mater. 29 (2017) 1603730. https://doi.org/10.1002/adma.201603730.

[8] P. Ren, X. Yang, Synthesis and Photo-Thermal Conversion Properties of Hierarchical Titanium Nitride Nanotube Mesh for Solar Water Evaporation, Sol. RRL. 2 (2018) 1700233. https://doi.org/10.1002/solr.201700233.

[9] P. Zhang, J. Li, L. Lv, Y. Zhao, L. Qu, Vertically Aligned Graphene Sheets Membrane for Highly Efficient Solar Thermal Generation of Clean Water, ACS Nano. 11 (2017) 5087–5093. https://doi.org/10.1021/acsnano.7b01965.

[10] H. Ghasemi, G. Ni, A.M. Marconnet, J. Loomis, S. Yerci, N. Miljkovic, G. Chen, Solar steam generation by heat localization, Nat. Commun. 5 (2014) 4449. https://doi.org/10.1038/ncomms5449.

[11] X. Zhou, F. Zhao, Y. Guo, Y. Zhang, G. Yu, A hydrogel-based antifouling solar evaporator for highly efficient water desalination, Energy Environ. Sci. 11 (2018) 1985–1992. https://doi.org/10.1039/C8EE00567B.

[12] Q. Chen, Z. Pei, Y. Xu, Z. Li, Y. Yang, Y. Wei, Y. Ji, A durable monolithic polymer foam for efficient solar steam generation, Chem. Sci. 9 (2018) 623–628. https://doi.org/10.1039/C7SC02967E.

[13] X. Li, J. Li, J. Lu, N. Xu, C. Chen, X. Min, B. Zhu, H. Li, L. Zhou, S. Zhu, T. Zhang, J. Zhu, Enhancement of Interfacial Solar Vapor Generation by Environmental Energy, Joule. 2 (2018) 1331–1338. https://doi.org/10.1016/j.joule.2018.04.004.

[14] X. Li, W. Xu, M. Tang, L. Zhou, B. Zhu, S. Zhu, J. Zhu, Graphene oxide-based efficient and scalable solar desalination under one sun with a confined 2D water path, Proc. Natl. Acad. Sci. 113 (2016) 13953–13958. https://doi.org/10.1073/pnas.1613031113.

[15] Z. Wang, W. Tu, Y. Zhao, H. Wang, H. Huang, Y. Liu, M. Shao, B. Yao, Z. Kang, Robust carbon-dot-based evaporator with an enlarged evaporation area for efficient solar steam generation, J. Mater. Chem. A. 8 (2020) 14566–14573. https://doi.org/10.1039/D0TA05179A.

[16] J. Yang, Y. Pang, W. Huang, S.K. Shaw, J. Schiffbauer, M.A. Pillers, X. Mu, S. Luo, T. Zhang, Y. Huang, G. Li, S. Ptasinska, M. Lieberman, T. Luo, Functionalized Graphene Enables Highly Efficient Solar Thermal Steam Generation, ACS Nano. 11 (2017) 5510–5518. https://doi.org/10.1021/acsnano.7b00367.

[17] S. Yu, Y. Zhang, H. Duan, Y. Liu, X. Quan, P. Tao, W. Shang, J. Wu, C. Song, T. Deng, The impact of surface chemistry on the performance of localized solar-driven evaporation system, Sci. Rep. 5 (2015) 13600. https://doi.org/10.1038/srep13600.

[18] Y. Shi, R. Li, Y. Jin, S. Zhuo, L. Shi, J. Chang, S. Hong, K.-C. Ng, P. Wang, A 3D Photothermal Structure toward Improved Energy Efficiency in Solar Steam Generation, Joule. 2 (2018) 1171–1186. https://doi.org/10.1016/j.joule.2018.03.013.

[19] C. Chen, Y. Li, J. Song, Z. Yang, Y. Kuang, E. Hitz, C. Jia, A. Gong, F. Jiang, J.Y. Zhu, B. Yang, J. Xie, L. Hu, Highly Flexible and Efficient Solar Steam Generation Device, Adv. Mater. 29 (2017) 1701756. https://doi.org/10.1002/adma.201701756.

[20] Y. Li, T. Gao, Z. Yang, C. Chen, W. Luo, J. Song, E. Hitz, C. Jia, Y. Zhou, B. Liu, B. Yang, L. Hu, 3D-Printed, All-in-One Evaporator for High-Efficiency Solar Steam Generation under 1 Sun Illumination, Adv. Mater. 29 (2017) 1700981. https://doi.org/10.1002/adma.201700981.

885 [21] P. Tao, G. Ni, C. Song, W. Shang, J. Wu, J. Zhu, G. Chen, T. Deng, Solar-driven
886 interfacial evaporation, Nat. Energy. 3 (2018) 1031–1041.
887 https://doi.org/10.1038/s41560-018-0260-7.

888 [22] X. Wu, G.Y. Chen, G. Owens, D. Chu, H. Xu, Photothermal materials: A key platform
889 enabling highly efficient water evaporation driven by solar energy, Mater. Today
890 Energy. 12 (2019) 277–296. https://doi.org/10.1016/j.mtener.2019.02.001.

891 [23] G. Wang, Y. Fu, A. Guo, T. Mei, J. Wang, J. Li, X. Wang, Reduced Graphene Oxide–
892 Polyurethane Nanocomposite Foam as a Reusable Photoreceiver for Efficient Solar
893 Steam Generation, Chem. Mater. 29 (2017) 5629–5635.
894 https://doi.org/10.1021/acs.chemmater.7b01280.

895 [24] Y. Li, T. Gao, Z. Yang, C. Chen, Y. Kuang, J. Song, C. Jia, E.M. Hitz, B. Yang, L. Hu,
896 Graphene oxide-based evaporator with one-dimensional water transport enabling high-
897 efficiency solar desalination, Nano Energy. 41 (2017) 201–209.
898 https://doi.org/10.1016/j.nanoen.2017.09.034.

899 [25] L. Shi, Y. Wang, L. Zhang, P. Wang, Rational design of a bi-layered reduced graphene
900 oxide film on polystyrene foam for solar-driven interfacial water evaporation, J. Mater.
901 Chem. A. 5 (2017) 16212–16219. https://doi.org/10.1039/C6TA09810J.

902 [26] P. Zhang, Q. Liao, T. Zhang, H. Cheng, Y. Huang, C. Yang, C. Li, L. Jiang, L. Qu, High
903 throughput of clean water excluding ions, organic media, and bacteria from defect-
904 abundant graphene aerogel under sunlight, Nano Energy. 46 (2018) 415–422.
905 https://doi.org/10.1016/j.nanoen.2018.02.018.

906 [27] P. Zhang, Q. Liao, H. Yao, H. Cheng, Y. Huang, C. Yang, L. Jiang, L. Qu, Three-
907 dimensional water evaporation on a macroporous vertically aligned graphene pillar array
908 under one sun, J. Mater. Chem. A. 6 (2018) 15303–15309.
909 https://doi.org/10.1039/C8TA05412F.

910 [28] L. Cui, P. Zhang, Y. Xiao, Y. Liang, H. Liang, Z. Cheng, L. Qu, High Rate Production
911 of Clean Water Based on the Combined Photo-Electro-Thermal Effect of Graphene
912 Architecture, Adv. Mater. 30 (2018) 1706805. https://doi.org/10.1002/adma.201706805.

913 [29] M. Zhu, Y. Li, F. Chen, X. Zhu, J. Dai, Y. Li, Z. Yang, X. Yan, J. Song, Y. Wang, E.
914 Hitz, W. Luo, M. Lu, B. Yang, L. Hu, Plasmonic Wood for High-Efficiency Solar Steam
915 Generation, Adv. Energy Mater. 8 (2018) 1701028.
916 https://doi.org/10.1002/aenm.201701028.

917 [30] H. Liu, C. Chen, G. Chen, Y. Kuang, X. Zhao, J. Song, C. Jia, X. Xu, E. Hitz, H. Xie, S.
918 Wang, F. Jiang, T. Li, Y. Li, A. Gong, R. Yang, S. Das, L. Hu, High-Performance Solar
919 Steam Device with Layered Channels: Artificial Tree with a Reversed Design, Adv.
920 Energy Mater. 8 (2018) 1701616. https://doi.org/10.1002/aenm.201701616.

921 [31] Z. Liu, H. Song, D. Ji, C. Li, A. Cheney, Y. Liu, N. Zhang, X. Zeng, B. Chen, J. Gao, Y.
922 Li, X. Liu, D. Aga, S. Jiang, Z. Yu, Q. Gan, Extremely Cost-Effective and Efficient
923 Solar Vapor Generation under Nonconcentrated Illumination Using Thermally Isolated
924 Black Paper, Glob. Chall. 1 (2017) 1600003. https://doi.org/10.1002/gch2.201600003.

925 [32] L. Wu, Z. Dong, Z. Cai, T. Ganapathy, N.X. Fang, C. Li, C. Yu, Y. Zhang, Y. Song,
926 Highly efficient three-dimensional solar evaporator for high salinity desalination by
927 localized crystallization, Nat. Commun. 11 (2020) 1–12. https://doi.org/10.1038/s41467-
928 020-14366-1.

[33] F. Zhao, X. Zhou, Y. Shi, X. Qian, M. Alexander, X. Zhao, S. Mendez, R. Yang, L. Qu, G. Yu, Highly efficient solar vapour generation via hierarchically nanostructured gels, Nat. Nanotechnol. 13 (2018) 489–495. https://doi.org/10.1038/s41565-018-0097-z.

[34] X. Li, G. Ni, T. Cooper, N. Xu, J. Li, L. Zhou, X. Hu, B. Zhu, P. Yao, J. Zhu, Measuring Conversion Efficiency of Solar Vapor Generation, Joule. 3 (2019) 1798–1803. https://doi.org/10.1016/j.joule.2019.06.009.

[35] H. Song, Y. Liu, Z. Liu, M.H. Singer, C. Li, A.R. Cheney, D. Ji, L. Zhou, N. Zhang, X. Zeng, Z. Bei, Z. Yu, S. Jiang, Q. Gan, Cold Vapor Generation beyond the Input Solar Energy Limit, Adv. Sci. 5 (2018) 1800222. https://doi.org/10.1002/advs.201800222.

[36] X. Wu, G.Y. Chen, W. Zhang, X. Liu, H. Xu, A Plant-Transpiration-Process-Inspired Strategy for Highly Efficient Solar Evaporation, Adv. Sustain. Syst. 1 (2017) 1700046. https://doi.org/10.1002/adsu.201700046.

[37] Q. Fang, T. Li, Z. Chen, H. Lin, P. Wang, F. Liu, Full Biomass-Derived Solar Stills for Robust and Stable Evaporation To Collect Clean Water from Various Water-Bearing Media, ACS Appl. Mater. Interfaces. 11 (2019) 10672–10679. https://doi.org/10.1021/acsami.9b00291.

[38] F. He, M. Han, J. Zhang, Z. Wang, X. Wu, Y. Zhou, L. Jiang, S. Peng, Y. Li, A simple, mild and versatile method for preparation of photothermal woods toward highly efficient solar steam generation, Nano Energy. 71 (2020) 104650. https://doi.org/10.1016/j.nanoen.2020.104650.

[39] M.M. Ghafurian, H. Niazmand, E. Ebrahimnia-Bajestan, R.A. Taylor, Wood surface treatment techniques for enhanced solar steam generation, Renew. Energy. 146 (2020) 2308–2315. https://doi.org/10.1016/j.renene.2019.08.036.

[40] T. Li, H. Liu, X. Zhao, G. Chen, J. Dai, G. Pastel, C. Jia, C. Chen, E. Hitz, D. Siddhartha, R. Yang, L. Hu, Scalable and Highly Efficient Mesoporous Wood-Based Solar Steam Generation Device: Localized Heat, Rapid Water Transport, Adv. Funct. Mater. 28 (2018) 1707134. https://doi.org/10.1002/adfm.201707134.

[41] C. Jia, Y. Li, Z. Yang, G. Chen, Y. Yao, F. Jiang, Y. Kuang, G. Pastel, H. Xie, B. Yang, S. Das, L. Hu, Rich Mesostructures Derived from Natural Woods for Solar Steam Generation, Joule. 1 (2017) 588–599. https://doi.org/10.1016/j.joule.2017.09.011.

[42] G. Xue, K. Liu, Q. Chen, P. Yang, J. Li, T. Ding, J. Duan, B. Qi, J. Zhou, Robust and Low-Cost Flame-Treated Wood for High-Performance Solar Steam Generation, ACS Appl. Mater. Interfaces. 9 (2017) 15052–15057. https://doi.org/10.1021/acsami.7b01992.

[43] C.-L. Guo, E.-D. Miao, J.-X. Zhao, L. Liang, Q. Liu, Paper-based integrated evaporation device for efficient solar steam generation through localized heating, Sol. Energy. 188 (2019) 1283–1291. https://doi.org/10.1016/j.solener.2019.07.023.

[44] A.K. Menon, I. Haechler, S. Kaur, S. Lubner, R.S. Prasher, Enhanced solar evaporation using a photo-thermal umbrella for wastewater management, Nat. Sustain. 3 (2020) 144–151. https://doi.org/10.1038/s41893-019-0445-5.

[45] H. Liu, C. Chen, H. Wen, R. Guo, N.A. Williams, B. Wang, F. Chen, L. Hu, Narrow bandgap semiconductor decorated wood membrane for high-efficiency solar-assisted water purification, J. Mater. Chem. A. 6 (2018) 18839–18846. https://doi.org/10.1039/C8TA05924A.

[46] Z. Li, M. Zheng, N. Wei, Y. Lin, W. Chu, R. Xu, H. Wang, J. Tian, H. Cui, Broadband-absorbing WO3-x nanorod-decorated wood evaporator for highly efficient solar-driven interfacial steam generation, Sol. Energy Mater. Sol. Cells. 205 (2020) 110254. https://doi.org/10.1016/j.solmat.2019.110254.

[47] W.-J. Liu, H. Jiang, H.-Q. Yu, Development of Biochar-Based Functional Materials: Toward a Sustainable Platform Carbon Material, Chem. Rev. 115 (2015) 12251–12285. https://doi.org/10.1021/acs.chemrev.5b00195.

[48] X. Xiao, B. Chen, Z. Chen, L. Zhu, J.L. Schnoor, Insight into Multiple and Multilevel Structures of Biochars and Their Potential Environmental Applications: A Critical Review, Environ. Sci. Technol. 52 (2018) 5027–5047. https://doi.org/10.1021/acs.est.7b06487.

[49] J.J. Lee, G. Engling, S.-C. Candice Lung, K.-Y. Lee, Particle size characteristics of levoglucosan in ambient aerosols from rice straw burning, Atmos. Environ. 42 (2008) 8300–8308. https://doi.org/10.1016/j.atmosenv.2008.07.047.

[50] Q. Zhang, L. Ren, X. Xiao, Y. Chen, L. Xia, G. Zhao, H. Yang, X. Wang, W. Xu, Vertically aligned Juncus effusus fibril composites for omnidirectional solar evaporation, Carbon. 156 (2020) 225–233. https://doi.org/10.1016/j.carbon.2019.09.067.

[51] J. Li, X. Zhou, P. Mu, F. Wang, H. Sun, Z. Zhu, J. Zhang, W. Li, A. Li, Ultralight Biomass Porous Foam with Aligned Hierarchical Channels as Salt-Resistant Solar Steam Generators, ACS Appl. Mater. Interfaces. 12 (2020) 798–806. https://doi.org/10.1021/acsami.9b18398.

[52] W. Fang, L. Zhao, X. He, H. Chen, W. Li, X. Zeng, X. Chen, Y. Shen, W. Zhang, Carbonized rice husk foam constructed by surfactant foaming method for solar steam generation, Renew. Energy. 151 (2020) 1067–1075. https://doi.org/10.1016/j.renene.2019.11.111.

[53] J. Fang, J. Liu, J. Gu, Q. Liu, W. Zhang, H. Su, D. Zhang, Hierarchical Porous Carbonized Lotus Seedpods for Highly Efficient Solar Steam Generation, Chem. Mater. 30 (2018) 6217–6221. https://doi.org/10.1021/acs.chemmater.8b01702.

[54] Y. Liao, J. Chen, D. Zhang, X. Wang, B. Yuan, P. Deng, F. Li, H. Zhang, Lotus leaf as solar water evaporation devices, Mater. Lett. 240 (2019) 92–95. https://doi.org/10.1016/j.matlet.2018.12.133.

[55] C. Sheng, N. Yang, Y. Yan, X. Shen, C. Jin, Z. Wang, Q. Sun, Bamboo decorated with plasmonic nanoparticles for efficient solar steam generation, Appl. Therm. Eng. 167 (2020) 114712. https://doi.org/10.1016/j.applthermaleng.2019.114712.

[56] Y. Lu, X. Wang, D. Fan, H. Yang, H. Xu, H. Min, X. Yang, Biomass derived Janus solar evaporator for synergic water evaporation and purification, Sustain. Mater. Technol. 25 (2020) e00180. https://doi.org/10.1016/j.susmat.2020.e00180.

[57] X. Wang, C. Sha, W. Wang, Y. Chen, Y. Yu, D. Fan, Functionalized biomass-derived composites for solar vapor generation, Mater. Res. Express. 6 (2019) 125613. https://doi.org/10.1088/2053-1591/ab586e.

[58] Y. Long, S. Huang, H. Yi, J. Chen, J. Wu, Q. Liao, H. Liang, H. Cui, S. Ruan, Y.-J. Zeng, Carrot-inspired solar thermal evaporator, J. Mater. Chem. A. 7 (2019) 26911–26916. https://doi.org/10.1039/C9TA08754K.

[59] C. Zhang, P. Xiao, F. Ni, L. Yan, Q. Liu, D. Zhang, J. Gu, W. Wang, T. Chen, Converting Pomelo Peel into Eco-Friendly and Low-Consumption Photothermic

Biomass Sponge Towards Multifunctional Solar-to-Heat Conversion, ACS Sustain. Chem. Eng. (2020). https://doi.org/10.1021/acssuschemeng.0c00681.

[60] N. Xu, X. Hu, W. Xu, X. Li, L. Zhou, S. Zhu, J. Zhu, Mushrooms as Efficient Solar Steam-Generation Devices, Adv. Mater. 29 (2017) 1606762. https://doi.org/10.1002/adma.201606762.

[61] S. Zhang, L. Zang, T. Dou, J. Zou, Y. Zhang, L. Sun, Willow Catkins-Derived Porous Carbon Membrane with Hydrophilic Property for Efficient Solar Steam Generation, ACS Omega. 5 (2020) 2878–2885. https://doi.org/10.1021/acsomega.9b03718.

[62] J. Li, M. Du, G. Lv, L. Zhou, X. Li, L. Bertoluzzi, C. Liu, S. Zhu, J. Zhu, Interfacial Solar Steam Generation Enables Fast-Responsive, Energy-Efficient, and Low-Cost Off-Grid Sterilization, Adv. Mater. 30 (2018) 1805159. https://doi.org/10.1002/adma.201805159.

[63] G.M. Hallegraeff, A review of harmful algal blooms and their apparent global increase, Phycologia. 32 (1993) 79–99. https://doi.org/10.2216/i0031-8884-32-2-79.1.

[64] L. Yang, G. Chen, N. Zhang, Y. Xu, X. Xu, Sustainable Biochar-Based Solar Absorbers for High-Performance Solar-Driven Steam Generation and Water Purification, ACS Sustain. Chem. Eng. 7 (2019) 19311–19320. https://doi.org/10.1021/acssuschemeng.9b06169.

[65] M. Zhu, A. Xia, Q. Feng, X. Wu, C. Zhang, D. Wu, H. Zhu, Biomass Carbon Materials for Efficient Solar Steam Generation Prepared from Carbonized Enteromorpha Prolifera, Energy Technol. n/a (2019) 1901215. https://doi.org/10.1002/ente.201901215.

[66] J. Li, X. Zhou, J. Zhang, C. Liu, F. Wang, Y. Zhao, H. Sun, Z. Zhu, W. Liang, A. Li, Migration Crystallization Device Based on Biomass Photothermal Materials for Efficient Salt-Rejection Solar Steam Generation, ACS Appl. Energy Mater. 3 (2020) 3024–3032. https://doi.org/10.1021/acsaem.0c00126.

[67] A. Celzard, A. Pasc, S. Schaefer, K. Mandel, T. Ballweg, S. Li, G. Medjahdi, V. Nicolas, V. Fierro, Floating hollow carbon spheres for improved solar evaporation, Carbon. 146 (2019) 232–247. https://doi.org/10.1016/j.carbon.2019.01.101.

[68] J. Zhou, Z. Sun, M. Chen, J. Wang, W. Qiao, D. Long, L. Ling, Macroscopic and Mechanically Robust Hollow Carbon Spheres with Superior Oil Adsorption and Light-to-Heat Evaporation Properties, Adv. Funct. Mater. 26 (2016) 5368–5375. https://doi.org/10.1002/adfm.201600564.

[69] S. Li, A. Celzard, V. Fierro, A. Pasc, Salting Effect in the Hydrothermal Carbonisation of Bioresources, ChemistrySelect. 1 (2016) 4161–4166. https://doi.org/10.1002/slct.201600837.

[70] N. Xu, J. Li, Y. Wang, C. Fang, X. Li, Y. Wang, L. Zhou, B. Zhu, Z. Wu, S. Zhu, J. Zhu, A water lily–inspired hierarchical design for stable and efficient solar evaporation of high-salinity brine, Sci. Adv. 5 (2019) eaaw7013. https://doi.org/10.1126/sciadv.aaw7013.

[71] A. Arenillas, J.A. Menéndez, G. Reichenauer, A. Celzard, V. Fierro, F.J. Maldonado Hodar, E. Bail$ó$n-Garcia, N. Job, Organic and Carbon Gels Derived from Biosourced Polyphenols, in: Org. Carbon Gels Lab. Synth. Appl., 2019: pp. 27–85. https://doi.org/10.1007/978-3-030-13897-4_2.

[72] L.I. Grishechko, G. Amaral-Labat, A. Szczurek, V. Fierro, B.N. Kuznetsov, A. Celzard, Lignin-phenol-formaldehyde aerogels and cryogels, Microporous Mesoporous Mater. 168 (2013) 19–29. https://doi.org/10.1016/j.micromeso.2012.09.024.

[73] N. Rey-Raap, A. Szczurek, V. Fierro, J.A. Menéndez, A. Arenillas, A. Celzard, Towards a feasible and scalable production of bio-xerogels, J. Colloid Interface Sci. 456 (2015) 138–144. https://doi.org/10.1016/j.jcis.2015.06.024.

[74] Y. Guo, X. Zhou, F. Zhao, J. Bae, B. Rosenberger, G. Yu, Synergistic Energy Nanoconfinement and Water Activation in Hydrogels for Efficient Solar Water Desalination, ACS Nano. 13 (2019) 7913–7919. https://doi.org/10.1021/acsnano.9b02301.

[75] X. Zhou, F. Zhao, Y. Guo, B. Rosenberger, G. Yu, Architecting highly hydratable polymer networks to tune the water state for solar water purification, Sci. Adv. 5 (2019) eaaw5484. https://doi.org/10.1126/sciadv.aaw5484.

[76] Y. Guo, H. Lu, F. Zhao, X. Zhou, W. Shi, G. Yu, Biomass-Derived Hybrid Hydrogel Evaporators for Cost-Effective Solar Water Purification, Adv. Mater. 32 (2020) 1907061. https://doi.org/10.1002/adma.201907061.

[77] D.P. Storer, J.L. Phelps, X. Wu, G. Owens, N.I. Khan, H. Xu, Graphene and Rice-Straw-Fiber-Based 3D Photothermal Aerogels for Highly Efficient Solar Evaporation, ACS Appl. Mater. Interfaces. (2020). https://doi.org/10.1021/acsami.0c01707.

[78] Q. Jiang, L. Tian, K.-K. Liu, S. Tadepalli, R. Raliya, P. Biswas, R.R. Naik, S. Singamaneni, Bilayered Biofoam for Highly Efficient Solar Steam Generation, Adv. Mater. 28 (2016) 9400–9407. https://doi.org/10.1002/adma.201601819.

[79] J. Jia, W. Liang, H. Sun, Z. Zhu, C. Wang, A. Li, Fabrication of bilayered attapulgite for solar steam generation with high conversion efficiency, Chem. Eng. J. 361 (2019) 999–1006. https://doi.org/10.1016/j.cej.2018.12.157.

[80] Y. Kuang, C. Chen, S. He, E.M. Hitz, Y. Wang, W. Gan, R. Mi, L. Hu, A High-Performance Self-Regenerating Solar Evaporator for Continuous Water Desalination, Adv. Mater. 31 (2019) 1900498. https://doi.org/10.1002/adma.201900498.

[81] Y. Zhang, S.K. Ravi, S.C. Tan, Systematic Study of the Effects of System Geometry and Ambient Conditions on Solar Steam Generation for Evaporation Optimization, Adv. Sustain. Syst. 3 (2019) 1900044. https://doi.org/10.1002/adsu.201900044.

[82] Z. Yu, S. Cheng, C. Li, Y. Sun, B. Li, Enhancing efficiency of carbonized wood based solar steam generator for wastewater treatment by optimizing the thickness, Sol. Energy. 193 (2019) 434–441. https://doi.org/10.1016/j.solener.2019.09.080.

[83] M. Zhu, Y. Li, G. Chen, F. Jiang, Z. Yang, X. Luo, Y. Wang, S.D. Lacey, J. Dai, C. Wang, C. Jia, J. Wan, Y. Yao, A. Gong, B. Yang, Z. Yu, S. Das, L. Hu, Tree-Inspired Design for High-Efficiency Water Extraction, Adv. Mater. 29 (2017) 1704107. https://doi.org/10.1002/adma.201704107.

[84] K.-K. Liu, Q. Jiang, S. Tadepalli, R. Raliya, P. Biswas, R.R. Naik, S. Singamaneni, Wood–Graphene Oxide Composite for Highly Efficient Solar Steam Generation and Desalination, ACS Appl. Mater. Interfaces. 9 (2017) 7675–7681. https://doi.org/10.1021/acsami.7b01307.

[85] B. Henderson- Sellers, A new formula for latent heat of vaporization of water as a function of temperature, Q. J. R. Meteorol. Soc. 110 (1984) 1186–1190. https://doi.org/10.1002/qj.49711046626.

[86] S. He, C. Chen, Y. Kuang, R. Mi, Y. Liu, Y. Pei, W. Kong, W. Gan, H. Xie, E. Hitz, C. Jia, X. Chen, A. Gong, J. Liao, J. Li, Z.J. Ren, B. Yang, S. Das, L. Hu, Nature-inspired salt resistant bimodal porous solar evaporator for efficient and stable water desalination, Energy Environ. Sci. 12 (2019) 1558–1567. https://doi.org/10.1039/C9EE00945K.